Peer-Reviewed Technical Communication

Sensitivity of Satellite Altimetry Data Assimilation on a Weapon Acoustic Preset

Peter C. Chu, Steven Mancini, Eric L. Gottshall, David S. Cwalina, and Charlie N. Barron

***Abstract*—The purpose of this research is to assess the benefit of assimilating satellite altimeter data for naval undersea warfare. To accomplish this, sensitivity of the weapon acoustic preset program (WAPP) for the Mk 48 variant torpedo to changes in the sound-speed profile (SSP) is analyzed with SSP derived from the modular ocean data assimilation system (MODAS). The MODAS fields differ in that one uses altimeter data assimilated from three satellites while the other uses no altimeter data. The metric used to compare the two sets of outputs is the relative difference in acoustic coverage area generated by WAPP. Output presets are created for five different scenarios, two antisurface warfare scenarios, and three antisubmarine warfare scenarios, in each of three regions: the East China Sea, Sea of Japan, and an area south of Japan that includes the Kuroshio currents. Analysis of the output reveals that, in some situations, WAPP output is very sensitive to the inclusion of the altimeter data because of the resulting differences in the subsurface predictions. The change in weapon presets can be so large that the effectiveness of the weapon may be affected.**

***Index Terms*—Antisubmarine warfare, antisurface warfare, modular ocean data assimilation system (MODAS), satellite altimetry data, weapon acoustic preset.**

I. Introduction

THE outcome of a battlefield engagement is often determined by the advantages and disadvantages held by each adversary. On the modern battlefield, the possessor of the best technology often has the upper hand, but only if that advanced technology is used properly and efficiently. To exploit this advantage and optimize the effectiveness of high-technology sensor and weapon systems, it is essential to understand the impact on them by the environment. In the arena of antisubmarine warfare (ASW), the ocean environment determines the performance of the acoustic sensors employed and the success of any associated weapon systems. Since acoustic sensors detect underwater sound waves, understanding how those waves propagate is crucial to knowing how the sensors will perform and being able to optimize their performance in a given situation. To gain this understanding, an accurate depiction of the ocean environment is necessary.

How acoustic waves propagate from one location to another under water is determined by many factors, some of which are described by the sound-speed profile (SSP). If the environmental properties of temperature and salinity are known over the entire depth range, the SSP can be estimated by using them in an empirical formula to calculate the expected sound speed in a vertical column of water. One way to determine these environmental properties is to measure them *in situ*, such as by conductivity–temperature–depth (CTD) or expendable bathythermograph (XBT) casts. This method is not always tactically feasible in the ASW scenario since the release of XBT will catch enemy's attention. Another method is to estimate the ocean conditions using a computer analysis tool, such as the modular ocean data assimilation system (MODAS) developed by the Naval Research Laboratory, Stennis Space Center, MI. MODAS assimilates *in situ* measurements such as XBT and remotely sensed data from satellites such as sea surface temperature (SST) from radiometers and sea surface height (SSH) from radar altimeters. MODAS represents real-time ocean thermohaline structure better than static climatology databases such as the U.S. Navy's generalized digital environmental model (GDEM) [7], [8], [4], and can improve the weapon acoustic weapon presets [5]. If MODAS provides an improved representation of actual ocean conditions when satellite altimetry data is assimilated, a MODAS field that has this information will differ from one that does not, especially in regions of high mesoscale activity. If these differences are large enough, a tactical decision aid may give very different sound-propagation characteristics depending on which MODAS field is used to represent the ocean environment. This, in turn, would cast doubt on predicted sensor performance and could render the technology ineffective, possibly changing the outcome of an engagement.

The purpose of this paper is to quantify the sensitivity of a naval ASW system, specifically the Mk 48 torpedo WAPP, to the assimilation of satellite altimetry data when MODAS is used as WAPP's source of SSP information. Since inclusion of SSH data is not always closely tied to relevant changes in SSP for weapon systems, and since it does not always represent an improvement in the predicted SSP, a convenient operational model MODAS is used to develop alternative SSPs and to validate the WAPP design and implementation. This is done by examining the relative difference (RD) in the output of WAPP when two

Manuscript received September 23, 2004; accepted January 4, 2006. This work was supported in part by the Space and Naval Warfare System Command, the Naval Undersea Warfare Center, Newport, RI, the Naval Research Laboratory, and the Naval Postgraduate School.

Associate Editor: L. Goodman.

P. C. Chu and S. Mancini are with the Naval Ocean Analysis and Prediction Laboratory, Department of Oceanography, Naval Postgraduate School, Monterey, CA 93943 USA (e-mail: pchu@nps.edu).

E. L. Gottshall is with the Space and Naval Warfare System Command, San Diego, CA 92110 USA.

D. S. Cwalina is with the Combat Control Systems Department, Naval Undersea Warfare Center, Newport, RI 02841 USA.

C. N. Barron is with the Naval Research Laboratory, Stennis Space Center, MI 39529 USA.

Color versions of one or more of the figures in this paper are available online at http://ieeexplore.ieee.org.

Digital Object Identifier 10.1109/JOE.2006.888869

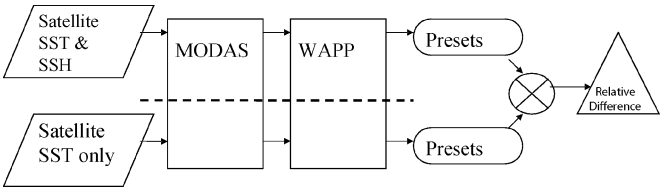

Fig. 1. Flow chart of the sensitivity study. Two MODAS SSP data sets with and without satellite altimeters are used for WAPP to generate two sets of weapon acoustic preset. Computing the relative difference between the two preset data sets gives the sensitivity of using satellite altimeters.

different MODAS fields are used as separate SSP inputs, as depicted in Fig. 1. The MODAS fields were identical in each case except that one has satellite altimetry data assimilated while the other does not [11].

If a significant degree of sensitivity is discovered, then the next logical step is to determine if the addition of satellite altimetry causes WAPP to respond more like it would have if *in situ* measurements were used as SSP input. This can be achieved in an experiment designed to compare WAPP output when MODAS fields and *in situ* measurements are used as separate SSP inputs. The question of how valuable this altimetry data is can then be more fully explored. On the other hand, if this paper shows little sensitivity to the different MODAS fields, then the value of satellite altimetry information, at least as an input to MODAS, can be assessed as low. Thus, this paper describes the WAPP validation. MODAS will strive to achieve the best SSP set possible because the variability of profiles and the sensitivity thresholds of other users have already demonstrated the need to consider SSH data, where appropriate.

II. MODAS

MODAS is one of the present U.S. Navy standard tools for production of 3-D grids of temperature and salinity. It is a modular system for ocean analysis and is built from a series of formula translator (FORTRAN) programs and Unix scripts that can be combined to perform desired tasks [5]. MODAS was designed to combine observed ocean data with climatological information to produce a quality-controlled, gridded analysis field as an output. The analysis uses an optimal interpolation (OI) data assimilation technique to combine various sources of data [7], [8], [13].

A. Static and Dynamic MODAS

MODAS has two modes of usage: static and dynamic MODAS. Static MODAS climatology is an internal climatology used as MODAS' first guess field. The other mode is referred to as the dynamic MODAS, which combines locally observed and remote sensed ocean data with climatological information to produce a near-real-time gridded 3-D analysis field of the ocean temperature and salinity structure as an output. Grids of MODAS climatological statistics range from 30-min resolution in the open ocean to 15-min resolution in shallow waters and 7.5-min resolution near the coasts in shallow water regions.

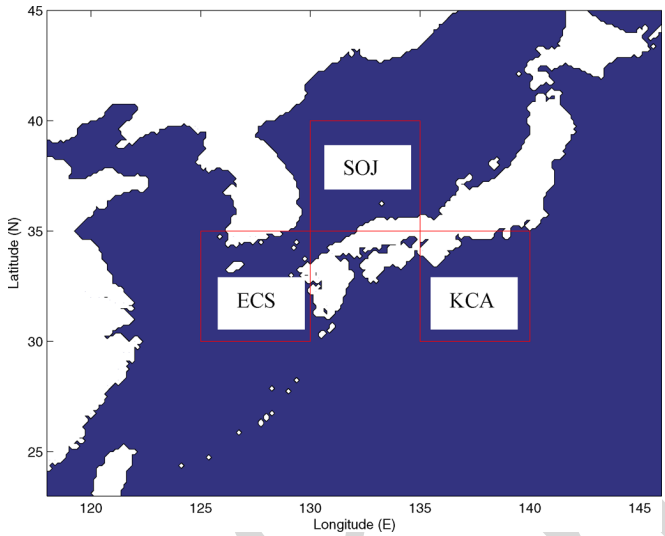

Fig. 2. Geographic regions selected for the study.

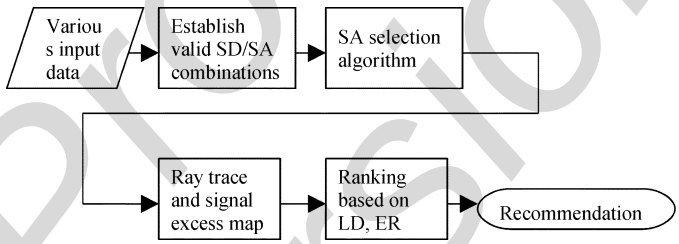

Fig. 3. Flow chart for illustrating the WAPP presetting procedure.

B. Synthetic Temperature and Salinity Profiles

Traditional oceanographic observations, such as CTD, XBT, etc., are quite sparse and irregularly distributed in time and space. It becomes important to use satellite data in MODAS for establishing real-time 3-D T/S ***[AU: Please define "T/S"]*** fields. Satellite altimetry and SST provide global data sets useful for studying ocean dynamics and for ocean prediction. MODAS has a component for creating synthetic temperature and salinity profiles [2], [1], which are the functions of parameters measured at the ocean surface such as satellite SST and SSH. These relationships were constructed using a least square regression analysis performed on archived historical database of temperature and salinity profiles (e.g., MOODS).

The following three steps are used to establish regression relationships between the synthetic profiles and satellite SST and SSH: 1) computing regional empirical orthogonal functions (EOFs) from the historical temperature and salinity profiles, 2) expressing the T/S profiles in terms of EOF series expansion, and 3) performing regression analysis on the profile amplitudes for each mode with the compactness of the EOF representation allowing the series to be truncated after only three terms while still retaining typically over 95% of the original variance [1].

C. First Guess Fields

The MODAS SST field uses the analysis from previous days field as the first guess, while the MODAS' 2-D SSH field uses a large scale weighted average of 35 d of altimeter data as a first

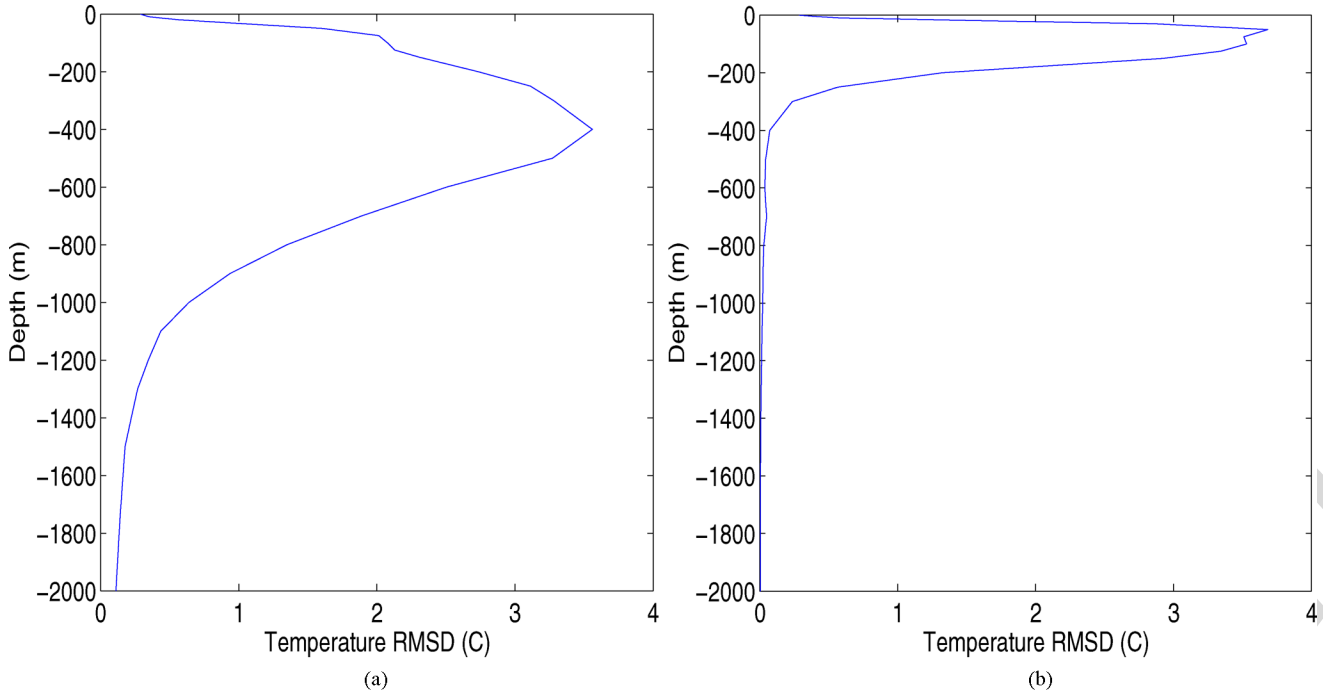

Fig. 4. Horizontal rmsd of MODAS temperature for (a) KCA and (b) SOJ on October 10, 2001.

TABLE I
VOLUME RMSD OF THE SIX MODAS FIELD PAIRS FOR SOUND SPEED (METER PER SECOND), TEMPERATURE (CELSIUS DEGREES), AND SALINITY (PRACTICAL SALINITY UNIT) IN 2001

	T (°C)	S (psu)	Sound Speed (m/s)
ECS Jun 30	1.12	0.81	1.12
KCA Jun 30	1.59	0.78	1.61
SOJ Jun 30	1.19	0.43	1.17
ECS Oct 10	1.04	0.58	1.16
KCA Oct 10	1.80	0.81	1.82
SOJ Oct 10	1.78	0.43	1.64

guess. The deviations calculated from the first guess field and the new observations are interpolated to produce a field of deviations from the first guess. Next, a final 2-D analysis is calculated by adding the field of deviations to the first guess field. When the model performs an optimum interpolation for the first time it uses the static MODAS climatology for the SST first guess field and zero for the SSH first guess field. Every day after the first optimum interpolation it uses previous day's first guess field for SST and a large scale weighted average is used for SSH. Synthetic profiles are generated at each location based on the last observation made at that location. If the remotely obtained SST and SSH for a location do not differ from the climatological data for that location, then climatology is used for that profile. If the remotely obtained SST and SSH for a location differ from the climatological data for that location then the deviation at each depth are estimated. Adding these estimated deviations to the climatology produces the synthetic profiles.

D. MODAS Fields With and Without Satellite Altimetry Data

Global MODAS fields are produced at the Naval Research Laboratory on a daily basis. The daily MODAS fields chosen for analysis are June 30, 2001 and October 10, 2001. For each day, there are two fields: one with altimetry data assimilated into it and one without altimetry data. The fields that included altimetry received the data from the three satellite systems having operational altimeters at the time: the National Aeronautics and Space Association (NASA's) TOPEX, the U.S. Navy's GEOSAT follow-on, and the European Space Agency's ERS-2 ***[AU: Please define "TOPEX", "GEOSAT" and "ERS"]***. To keep the data analysis manageable, but at the same time to gather a large enough number of data comparison points, three geographic regions, each five-by-five degrees in latitude and longitude, were cut out of the MODAS fields for each day. The boxes, shown in Fig. 2, are located in the East China Sea region (ECS, 30°–35° N, 125°–130° E), the Sea of Japan region (SOJ, 35°–40° N, 130°–135° E), and the Kuroshio Current area south of Japan (KCA, 30°–35° N and 135°–140° E), and are chosen for their varying amounts of mesoscale variability as well as their tactical significance. Segregating these regions by the two dates created six MODAS cases to analyze. These MODAS (T/S) fields are taken as input for the acoustic ray tracing model in the Weapon Acoustic Preset Program (WAPP) to determine suggested presets for a Mk 48 variant torpedo.

The resolution of MODAS in these regions is one eighth of a degree, which yielded three grids of 41-by-41 points each. After eliminating grid points over areas of land, the number of vertical profiles made available to WAPP for each case is as follows: 1495 pairs for SOJ,; 1448 pairs for ECS, and 1436 pairs for KCA, for a total of 4379 pairs of profiles. Each vertical profile pair is for the same location and day, but each is taken from the two different versions of MODAS fields. The output of WAPP can, therefore, be compared using each pair of vertical profiles to determine the sensitivity of the output to the altimetry data.

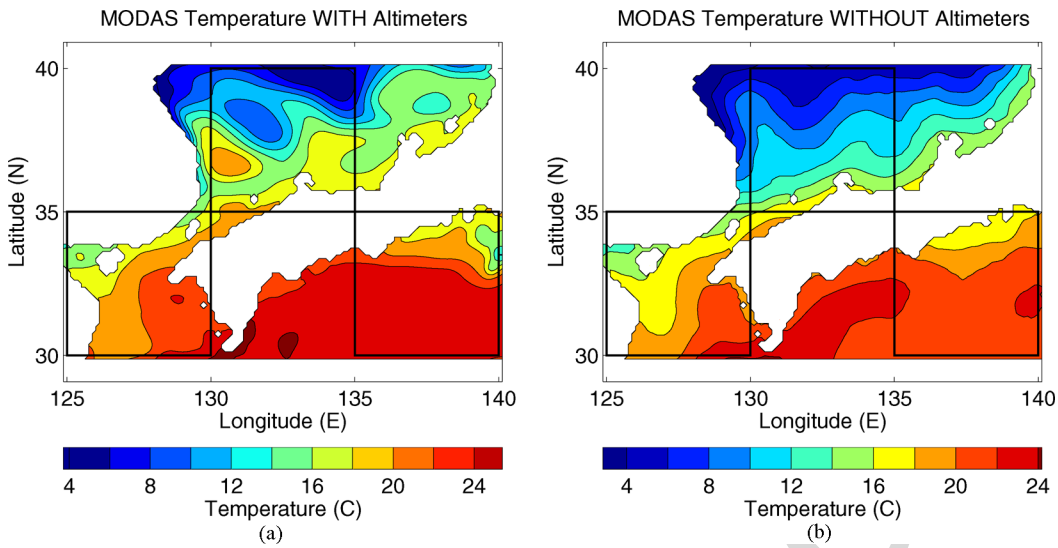

Fig. 5. Comparison between MODAS temperature at 100 m on October 10, 2001 (a) with and (b) without satellite altimetry data assimilated. Here, the upper middle box is used for the SOJ evaluation, the lower right box is used for the KCA evaluation, and lower left box is used for the ECS evaluation (see Fig. 2).

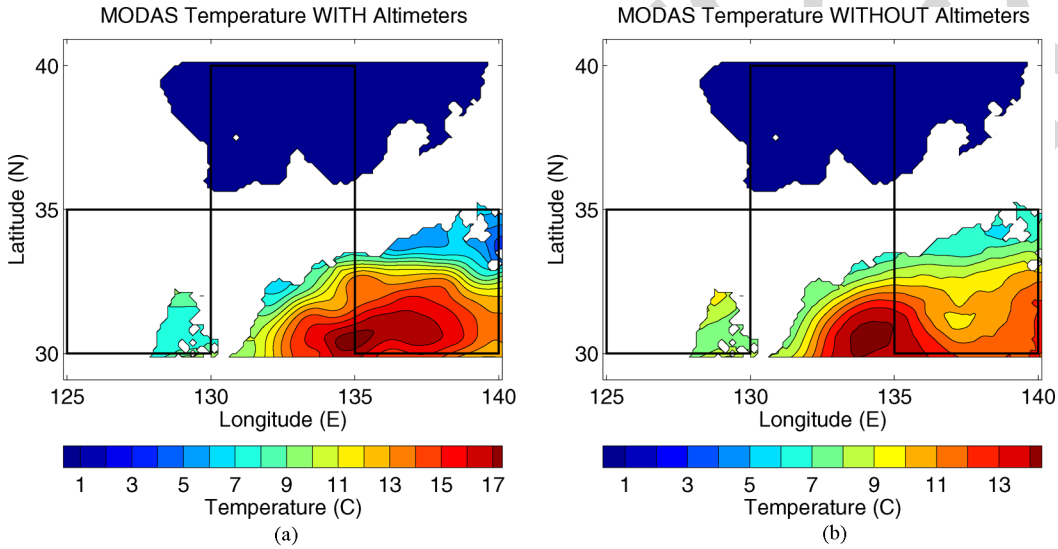

Fig. 6. Comparison between MODAS temperature at 500 m on October 10, 2001 (a) with and (b) without satellite altimetry data assimilated. Here, the upper middle box is used for the SOJ evaluation, the lower right box is used for the KCA evaluation, and lower left box is used for the ECS evaluation (see Fig. 2).

III. WAPP

A. General Description

WAPP is an automated, interactive program designed to provide the fleet with an onboard means of generating acoustic presets for multiple variants of Mk 48 torpedoes and visualizing their performance. Developed by the Naval Undersea Warfare Center (NUWC, Division Newport, RI), it consists of several elements including a graphical user interface (GUI) for entering various data, a computational engine for generating acoustic performance predictions, and various forms of output (NUWC, 2004***[AU: What are you referreing to here?]***).

The types of necessary input data include tactical (such as tactic type and depth zone of interest), target (such as acoustic and Doppler characteristics), weapon (such as type, mod, and active or passive acoustic mode), and environmental information. To input the environmental information, the user selects the "environment" pull-down menu of the GUI to bring up the environmental data entry (EDE) window. This window allows the entry of water-column parameter profiles (such as temperature, salinity, sound speed, and volume scattering strength) for a specified latitude and longitude. Other environmental input entered via the EDE consists of sea surface conditions (wind speed, waveheight, and sea state) and bottom conditions (depth and type). Operationally, the environmental data is received from the sonar tactical decision aid.

B. WAPP Presetting Process

Once the necessary information is input (or default values are selected), WAPP is ready to undergo the presetting process. This process is begun by using the "compute" pull-down menu of the GUI and is outlined in Fig. 3. The first step is to establish a valid set of search depth (SD) and search angle (SA)

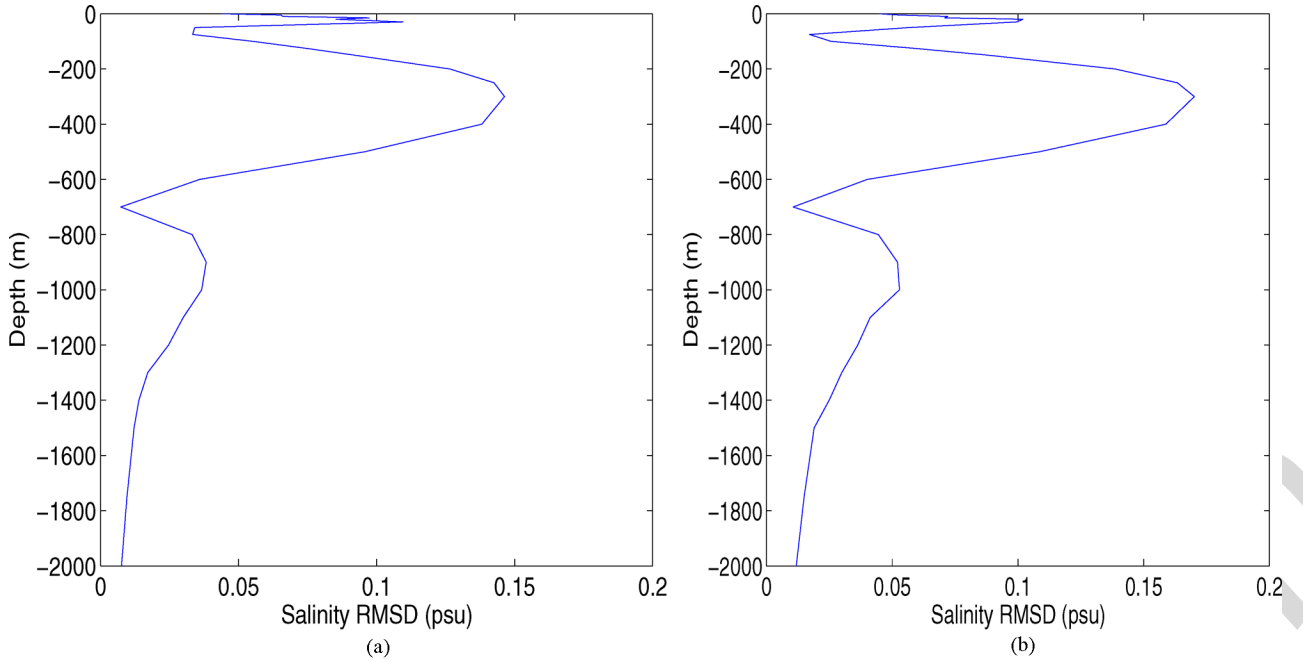

Fig. 7. Horizontal rmsd of MODAS salinity for KCA on (a) June 30, 2001 and (b) October 10, 2001.

combinations. The program then invokes an SA selection algorithm to identify the optimal pitch angle for each SD. Next, the computational engine traces, in a series of time steps, a fan of rays that bound the torpedo beam pattern for each resulting SD/SA combination (NUWC, 2004***[AU: Which reference is this?]***). A signal excess computation is performed and mapped to a gridded search region at each time step using the monostatic, active sonar equation for the reverberation limited case

$$\mathrm{SL} - 2\mathrm{TL} + \mathrm{TS} - \mathrm{RL} - \mathrm{DT} = \mathrm{SE} \tag{1}$$

where

SL	active sonar source level;
TL	two-way transmission loss between the sonar and the target;
TS	target strength;
RL	reverberation level;
DT	detection threshold.

The signal excess map is used to determine the effectiveness ratio (the fraction of the prosecutable search region with signal excess greater than 0 dB, also called area coverage) and laminar distance (the location of signal excess center of mass). Then, WAPP ranks the SD/SA combinations based on these computations (along with some other mitigating factors) and makes a recommendation as to the best preset for the given scenario.

In solving (1), the SL, DT, and TS terms are based on properties of the sonar system and target involved, so they are selected by the program or entered by the user, as is the case for TS. The TL and RL terms are computed using a range-independent, ray theory propagation model that accounts for geometric spreading, refractive effects, volumetric effects, and boundary interactions with the ocean surface and bottom. The vertical SSPs used by the ray tracing model are calculated by WAPP from the temperature and salinity profiles using the equation proposed by Chen and Millero [3]. Geometric spreading and refractive losses are determined using the transmission loss equation derived using ray theory

$$\mathrm{TL} = 10\log\left(\frac{R_k\left|\frac{\partial R_k}{\partial \theta_o}\sin\theta_k\right|}{\cos\theta_o}\right) \tag{2}$$

where R_k is the horizontal range at some position downrange, θ_o is the initial angle of the ray, and θ_k is the angle of the ray at range R_k. Volume absorption is introduced into the transmission loss term using absorption coefficients calculated from the chemical relaxation method proposed by Francois and Garrison [9], [10].

C. Ranked List Set

To offer a means of user interaction, the output of WAPP is in the form of a ranked list set of SDs, pitch angles, laminar distances, and effectiveness values. This allows the user to view all SD/SA combinations, not just the recommended one, and select the most appropriate one for the situation. The list set is, therefore, a list of possible presetting choices from which the operator can choose. In addition, the ray traces and signal excess maps are viewable using the GUI's "acoustic coverage" pull-down menu. These forms of output provide a visual interpretation of the acoustic performance of the torpedo, including boundary interactions and refraction effects.

Since the propagation model uses ray theory, it has all the shortcomings associated with it, such as being limited to higher frequencies. In this case, this is an acceptable condition because

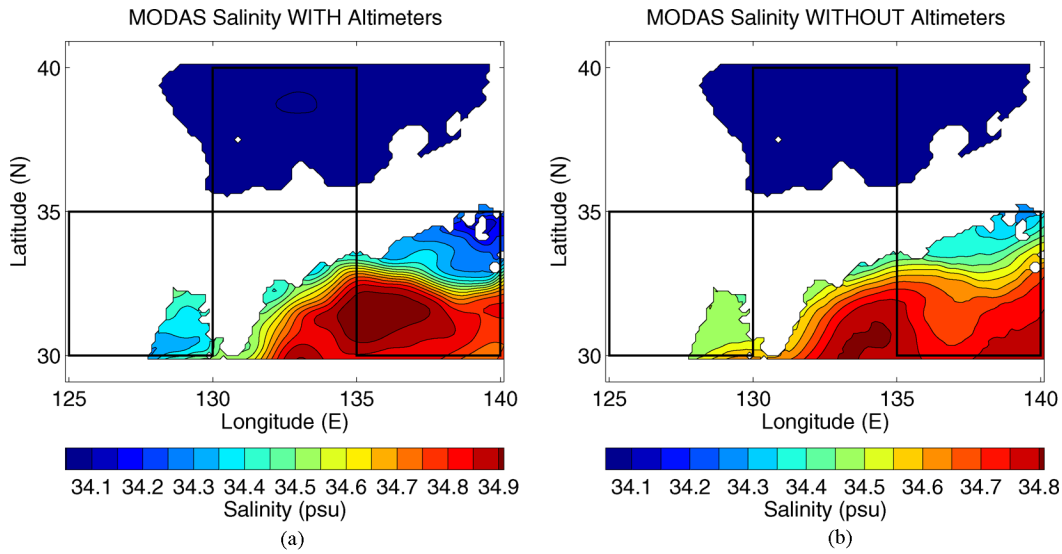

Fig. 8. Comparison between MODAS salinity at 300 m on June 30, 2001 (a) with and (b) without satellite altimetry data assimilated. Here, the upper middle box is used for the SOJ evaluation, the lower right box is used for the KCA evaluation, and lower left box is used for the ECS evaluation (see Fig. 2).

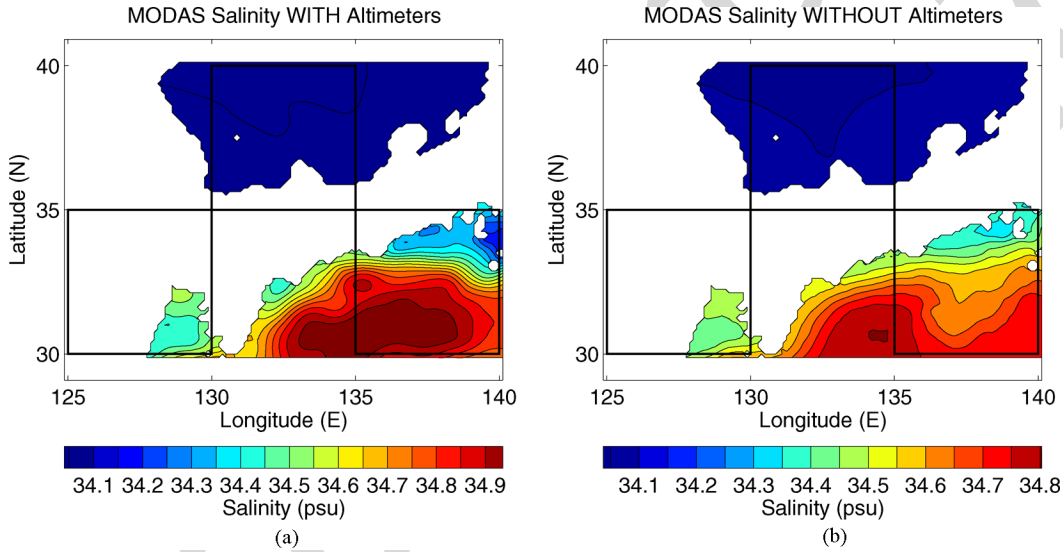

Fig. 9. Comparison between MODAS salinity at 300 m on October 10, 2001 (a) with and (b) without satellite altimetry data assimilated. Here, the upper middle box is used for the SOJ evaluation, the lower right box is used for the KCA evaluation, and lower left box is used for the ECS evaluation (see Fig. 2).

the Mk 48 torpedo has a suitably high operating frequency. Another deficiency of ray theory is the poor handling of shadow zones due to the assumption that no acoustic energy leaks out of the ray tube. This is also acceptable because, from a weapon presetting standpoint, it is unrealistic to direct a torpedo home on a target in a shadow zone, so an accurate description of the sound field is not necessary***[AU: Sentence was changed. Please check.]***. Finally, ray theory has the issue of causing energy to approach infinity at caustics and turning points. This last concern is mitigated through the use of a caustic correction that modifies the propagation equations, thereby avoiding the case where the denominator becomes zero, and approximates the signal level near the caustic.

Because the propagation model is range independent, it assumes cylindrical symmetry, meaning it does not have range-varying properties. The resulting ray traces are assumed to be valid for any direction from the source location, as the model environment looks the same down any bearing [6], [12]. This is not ideal for determining accurate sound-propagation characteristics, especially in regions where the oceanography changes rapidly with horizontal distance, and can affect the weapon presets. Under less variable conditions, this shortcoming would probably have little or no affect on the weapon presets, as the typical Mk 48 torpedo engagement would only involve a few kilometers of ocean. Regardless, there is an effort currently underway to utilize the comprehensive acoustic sonar simulation for range-dependent performance predictions for torpedo presetting. The assumption of range independence is consistent with areas where there is little to no bathymetric variation over torpedo detection ranges and also with cross-slope predictions in more variable environments. Here, it provides a reasonable

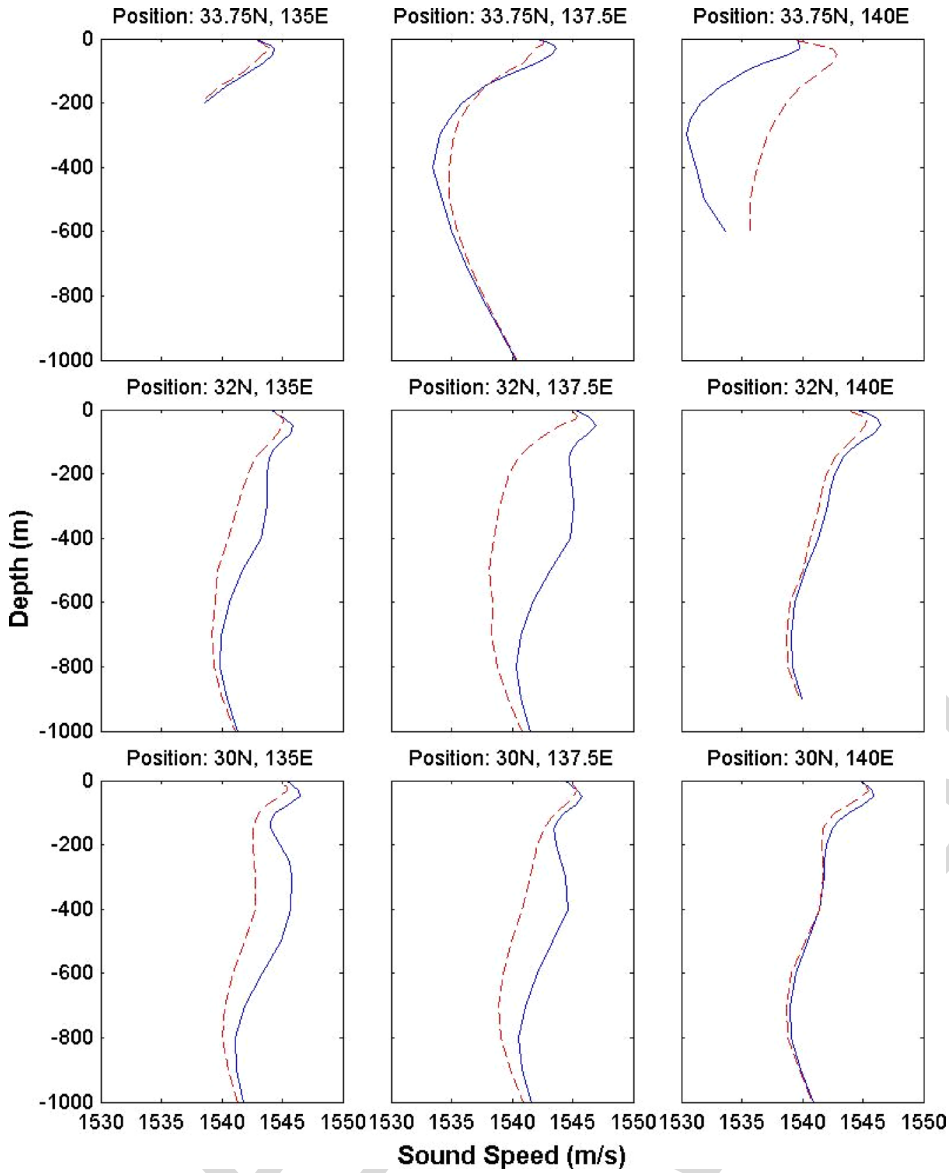

Fig. 10. Comparison of MODAS SSPs for KCA on October 10, 2001 with and without satellite altimetry data assimilated. Here, the solid curves are SSPs with altimeters and the dashed curves are SSPs without altimeters.

assessment of the importance of satellite altimetry data using the current weapon system.

IV. Numerical Simulations

The MODAS temperature and salinity fields were fed into WAPP. Then, WAPP performed its presetting process for each MODAS grid point using the vertical profile data for each location. Grid points over land had no vertical profiles, of course, and are discarded. The vertical SSP is calculated by WAPP from the temperature and salinity profiles, as opposed to using the SSP available from the MODAS field. The same default values for volume scattering strength and surface and bottom roughness/reflectivity were used for each run. This procedure is repeated for the two MODAS field versions (with and without satellite altimetry data), for both days, for each geographic region, and for the five tactical scenarios. The tactical scenarios are prescribed using the GUI to change the tactic ("surface craft" for the ASUW ***[AU: Please define "ASUW"]*** scenarios, "unknown sub" for the ASW scenarios), the target maximum depth (15 m for the ASUW scenarios, 213 m for the shallow ASW scenarios, and 396 m for the deep ASW scenarios), and the target Doppler ("low" for the low Doppler scenarios, "high" for the high Doppler scenarios).

Since one list set is produced for each profile and five different tactical scenarios are integrated for each case, five times as many list sets are produced as there are MODAS profiles. These list sets can be considered as pairs, just as the vertical profiles are; one pair for each location, day, and tactical scenario, each being comprised of one list set for each of the two MODAS field versions. To compare each pair of list sets, a configuration management program and its included statistical software package are employed. This program is actually designed to check WAPP output for differences during verification testing upon completion of software upgrades. In that application, the input is held

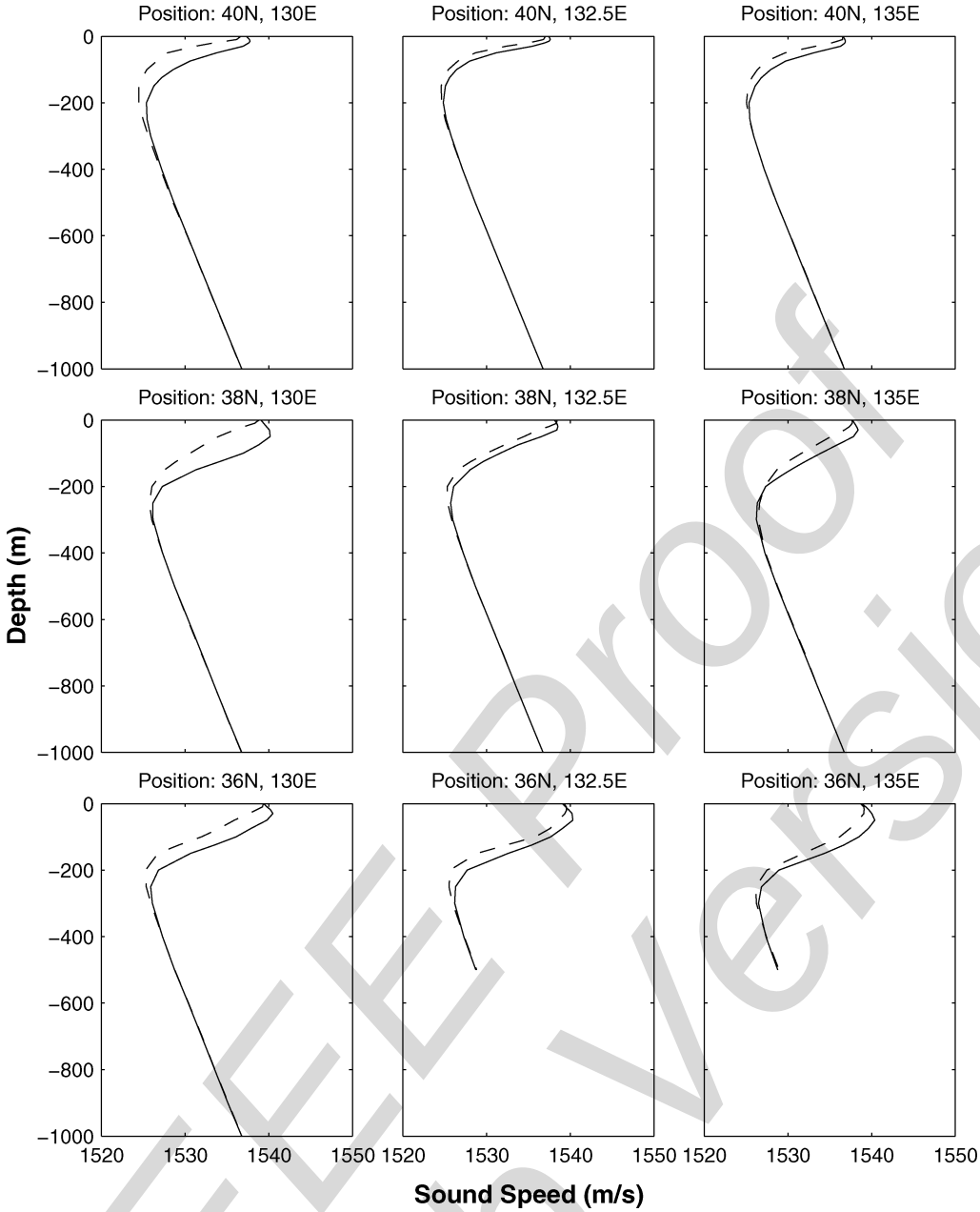

Fig. 11. Comparison of MODAS SSPs for SOJ on October 10, 2001 with and without satellite altimetry data assimilated. Here, the solid curves are SSPs with altimeters and the dashed curves are SSPs without altimeters. The use of SSH data by MODAS introduced only small changes in the SOJ SSPs at weapon/target depths relative to the changes witnessed in the KCA area for the same time period (see Fig. 10). This is a result of larger rmsd of temperature in the KCA than in SOJ especially at depths deeper than 400 m (see Fig. 4).

constant between the two WAPP software versions, so any differences in output are due to software changes (the aim is to have no differences). For the current application, the input was varied and the WAPP version was held constant. Therefore, any differences in the output can be attributed to differences in the input.

V. Statistical Analysis

A. Input and Output Differences

The difference of the two sets of input MODAS with and without satellite altimetry data $(X_1^{(\mathrm{in})}, X_2^{(\mathrm{in})})$ and the two sets of output weapon preset data using MODAS with and without satellite altimetry data $(X_1^{(\mathrm{out})}, X_2^{(\mathrm{out})})$

$$\Delta X = X_1 - X_2$$

represent the ocean data update using satellite altimetry data (input) and the effect of using satellite altimetry data on the weapon preset (output). Here, X_1 and X_2 are the variables (either input or output) using MODAS with and without satellite altimetry data, respectively. The difference was calculated at each horizontal grid point and depth. Besides histograms and scatter diagrams of the two sets of input and output data, bias

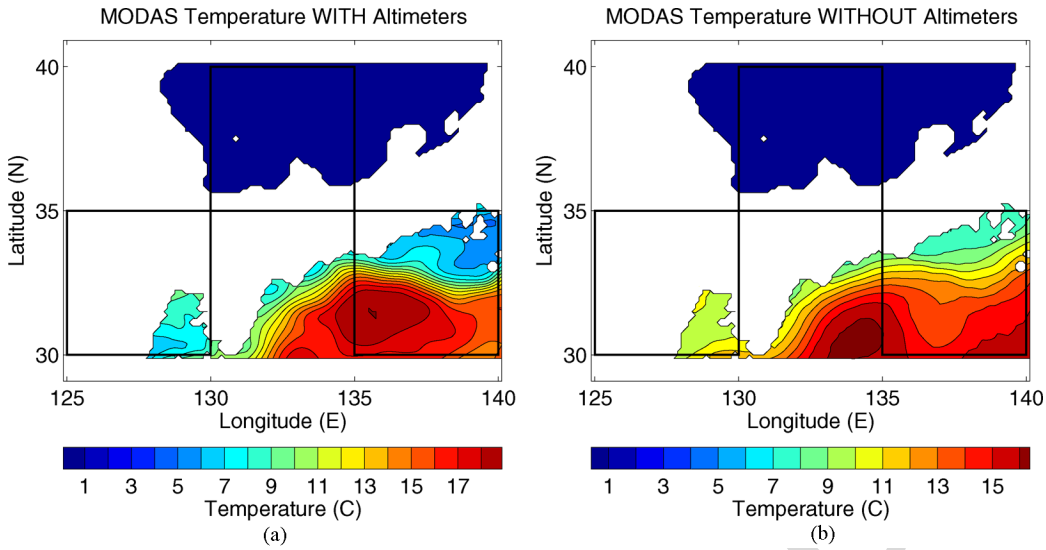

Fig. 12. Comparison between MODAS salinity at 400 m on June 30, 2001 (a) with and (b) without satellite altimetry data assimilated. Here, the upper middle box is used for the SOJ evaluation, the lower right box is used for the KCA evaluation, and lower left box is used for the ECS evaluation (see Fig. 2).

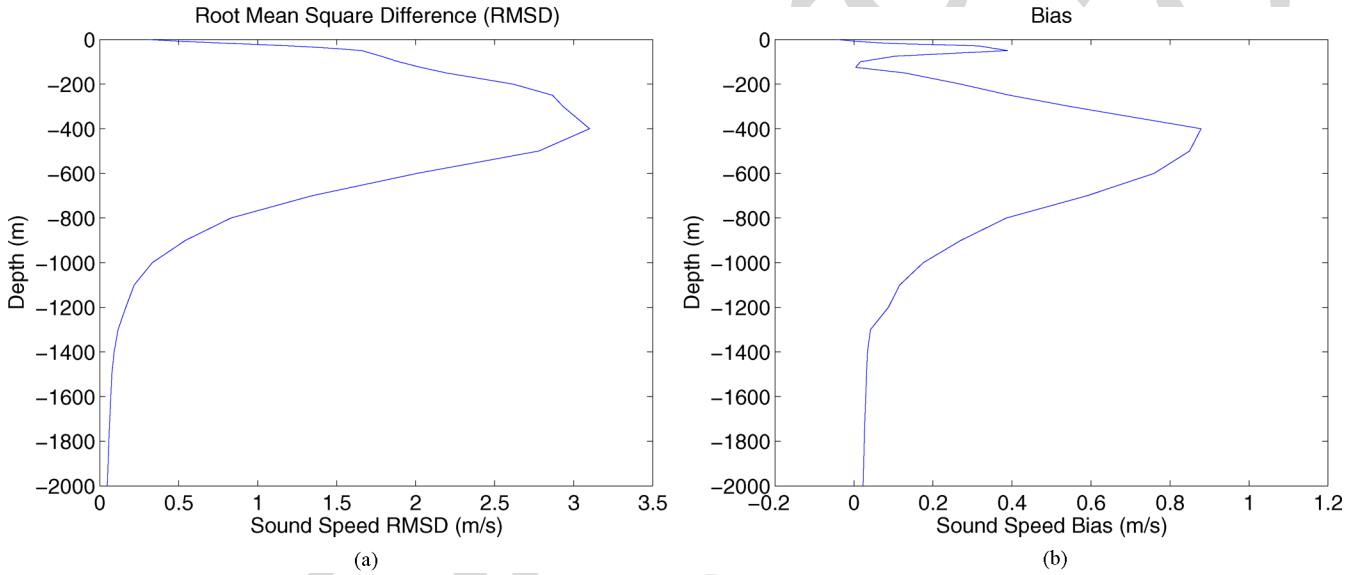

Fig. 13. (a) Horizontal rmsd and (b) bias of MODAS SSP for KCA on June 30, 2001.

and root-mean-square difference (rmsd) are often used. The bias is represented by the mean of the following differences:

$$\Delta\overline{X} = \frac{1}{n}\sum_{i=1}^{n}\Delta X_i \tag{3}$$

and the overall difference is represented by the rmsd

$$\text{rmsd} = \sqrt{\frac{1}{n}\sum_{i=1}^{n}\Delta X_i^2}. \tag{4}$$

Bias and rmsd can be computed over volume (called volume rmsd) or over a horizontal plane (called horizontal rmsd).

B. *Probability of Relative Difference Over a Threshold*

The statistical package produced absolute values of the relative differences (RD) in area coverage (AC) for different SD/SA combination

$$\text{RD} = \frac{|\text{AC}_1 - \text{AC}_2|}{\text{AC}_1}. \tag{5}$$

Here, the subscripts 1 and 2 denote MODAS with and without satellite altimetry data.

The presetting process has generated pairs of list sets in which some SD/SA combinations were the same and some were different. The list set can be thought of as a list of presetting choices; the choices on one list sometimes match those on the other list and sometimes they do not. The instances in which WAPP produce different SD/SA combinations for a profile pair are the cases in which an actual engagement will have greater

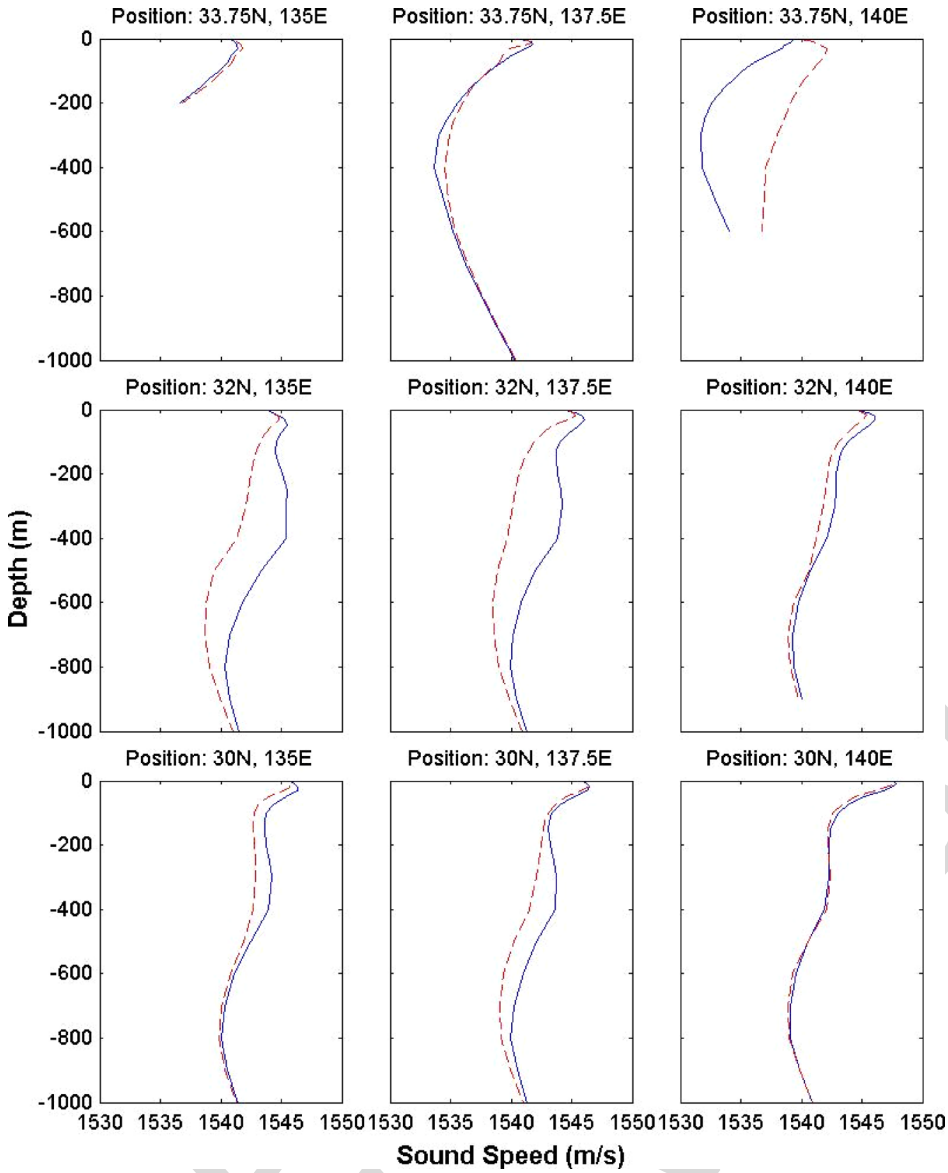

Fig. 14. Comparison of MODAS SSP for KCA on June 30, 2001 with and without satellite altimetry data assimilated. Here, the solid curves are SSPs with altimeters and the dashed curves are SSPs without altimeters.

potential for a different outcome because, given these different choices, the torpedo will not be searching at the same depth, looking at the same SA, or both. Determining the sensitivity of WAPP to input differences in these cases is important because of the potential for weapon effectiveness to be affected. The thing to be aware of here is that the actual environment is whatever it is, regardless of differences in the MODAS fields. In the cases where the same SD/SA combinations (same choices) are generated for the two MODAS versions, the outcome of the engagement will be very similar, subject to other targeting considerations, because the same presets and environment are involved.

Histogram of RD displays the number of different SD/SA combinations with area coverage relative differences in specified ranges, or bins. The probabilities of RD being greater than 0.1, 0.2, and 0.5

$$\mu_1 = \mathrm{Prob}(\mathrm{RD} > 0.1)$$
$$\mu_2 = \mathrm{Prob}(\mathrm{RD} > 0.2)$$
$$\mu_3 = \mathrm{Prob}(\mathrm{RD} > 0.5) \quad (6)$$

are used for the determination of the sensitivity.

VI. Comparison Between Two MODAS Data Sets

A. Volume rmsd

The volume rmsd values (Table I) indicate overall difference in the MODAS analyses for each case. The largest differences in the temperature fields occurred in KCA on both days and in SOJ on October 10, 2001, where the volume rmsd values ranging from 1.58 °C to 1.80 °C. The other cases have rmsd values of 1.18 °C or less. Salinity differences are also largest in KCA on both days, but ECS on June 30, 2001 had large volume salinity rmsd as well. These three cases have values ranging from 0.0759 to 0.0822 psu, whereas the other cases have values of 0.056 psu or less. The derived sound-speed analyses closely followed

the temperature fields, which is to be expected as temperature ranges often have the largest affect on sound speed. The largest values of the sound-speed volume rmsd range from 1.62 to 1.84 m/s and occur in the same cases as they do for the temperature analyses. The remaining cases have values of 1.15 m/s and smaller.

B. Horizontal rmsd

1) MODAS on October 10, 2001: The vertical profiles of horizontal rmsd allow for a more detailed comparison by showing at what depths the largest average differences occurred for each case. The largest differences in the temperature analyses occurred in the October 10 profiles for KCA and SOJ. Both have horizontal rmsd values of well over 3 °C at different depths, as shown in Fig. 4. The maximum values in the KCA profile occur between 300 and 500 m, whereas in the SOJ profile they are in the 50–200-m range.

A comparison of the horizontal temperature fields on October 10, 2001 at 100 m (Fig. 5) and 500 m (Fig. 6) lends some explanation for the high rmsd values in these cases. The panel with altimeter data in Fig. 5 reveals a subsurface eddy system, comprised of both a warm-core and a cold-core eddy, and a stronger polar front in SOJ; eddies are noticeably absent from the panel without altimeter data. The panel with altimeter data in Fig. 6 shows a much stronger subsurface front in KCA, including cooler water to the north and warmer water to the south of the front, than the panel without altimeter data does.

The largest differences in the salinity analyses occur in the KCA profiles on both days. They have horizontal rmsd values of about 0.15 psu or more, with maximum values in the 200–400-m range, as shown in Fig. 7. The horizontal salinity fields at 300 m are shown in Figs. 8 and 9. Similar to the temperature field shown previously, a much stronger front is depicted in the panel with altimetry data, with a larger contrast in salinity on either side of the front. This is true for both days.

As is to be expected, the horizontal rmsd for SSP looks very similar to that for temperature. It follows, then, that the largest values of well over 3 m/s occur in the October 10 profiles for KCA and SOJ at the same depth ranges as the temperature profiles: 300–500 m in the KCA profile and 50–200 m in the SOJ profile.

The horizontal rmsd previously discussed helps to explain the SSP pattern observed for each case. Figs. 10 and 11 illustrate this well for the two cases with the largest differences in the sound-speed (and temperature) MODAS analyses, the October 10 fields for KCA and SOJ. The nine SSP pairs in each figure are displayed so that their positions correspond to their locations within the area. For example, the top left panel shows the SSP pair for a location in the northwest portion of the box; the center panel is for a location near the center of the box, and so on. (Note: the horizontal scale may change from panel to panel, so care must be taken to understand the relative changes between panels.) This type of display provides the additional information of horizontal positioning of the largest differences as well as their depths.

The largest deviations found in the SSP pairs (Fig. 10) correspond to the depth zone already identified as having the largest rmsd values for KCA on October 10, that being 300–500 m. The top-right, center, and two bottom-left panels show the most deviation and correspond to the locations of the largest temperature differences in Fig. 6. The top three panels are profiles from within the front, showing the stronger gradient discovered earlier for the field with altimetry than for the one without. These stronger gradients produce the stronger sound channels evident in the right two panels. The middle and bottom panels show the result of the field with altimetry having much warmer water to the south of the front: the sound speeds are much faster there. They also show more of a gradient in the nonaltimetry field; a result of that field depicting a more spread out front than the tightly packed, stronger front of the altimetry field. Another obvious difference in the center and two bottom-left panels is the second, shallow sound channel in the altimetry field profiles, where one does not exist (or is very weak) in the nonaltimetry field.

Looking now at SOJ on October 10, shown in Fig. 11, the largest deviations in the SSP pairs are seen in the left most panels in the upper 200 m, corresponding to where the eddy system is located in Fig. 5. In all the panels, for the most part, the altimetry profiles show higher sound speeds in the upper 300 m or so, this mostly being due to the prevalent warmer temperatures in the altimetry field there. Very noticeable in the middle and bottom panels is a more pronounced sonic layer at the surface in the altimetry fields, corresponding to the existence of, or a deeper, mixed layer.

2) MODAS on June 30, 2001: Just like on October 10, 2001 (Fig. 6), the temperature field on June 30, 2001 shows a much stronger subsurface front as well as cooler water to the north and warmer water to the south of the front in the MODAS temperature field with altimetry [Fig. 12(a)] than without altimetry [Fig. 12(b)]. The salinity field with altimetry (Fig. 8) also indicates the existence of a stronger front. The largest rmsd of SSP and bias values exist in a band from about 100 to 600 m on June 30, 2001 (Fig. 13). The MODAS SSPs on June 30, 2001 (Fig. 14) illustrate characteristics similar to the SSPs for KCA on October 10, 2001 (Fig. 10).

VII. Comparison of Weapon Acoustic Preset Pairs

The differences in the MODAS fields may have an effect on the output of WAPP, depending on the sensitivity of WAPP to changes in input. The cases highlighted here have fairly significant differences in the temperature, salinity, and sound-speed fields. For the most part, in each of the 30 scenario histograms, the number of different SD/SA combinations dropped off with increasing RD. In other words, the peak RD was usually in the lowest bin (less than 0.05) and decreased with each successive bin in a decaying fashion, as illustrated by Fig. 15(a). The most notable exceptions are the two ASUW tactics for the SOJ October case, which have peaks in the bin for 0.3–0.4, one of which is shown in Fig. 15(b). The next two figures ***[AU: Please specify which figures]*** display collectively some of the values determined for each histogram, including μ_1 and μ_2 (i.e., the probabilities of the RD being greater than 0.1 and 0.2) and mean RD. The results are grouped by case and broken down into each tactic.

The general trend for each case (except for SOJ on June 30, 2001) is for the probability values to decrease with increasing

TABLE II
OVERALL SENSITIVITY OF WEAPON ACOUSTIC PRESET TO ALTIMETRY DATA ASSIMILATION USING MODAS

Scenario	Prob(RD > 0.1)	Prob(RD > 0.2)	Prob(RD > 0.5)	Mean RD
ECS Jun HD Deep ASW	17.51	2.64	0.00	0.0618
ECS Jun LD Deep ASW	21.82	4.10	0.00	0.0725
ECS Jun LD Shallow ASW	21.77	3.65	0.00	0.0723
ECS Jun HD ASUW	39.59	19.63	0.28	0.1110
ECS Jun LD ASUW	26.29	9.45	0.06	0.0818
KCA Jun HD Deep ASW	39.26	6.63	0.00	0.0924
KCA Jun LD Deep ASW	37.52	6.44	0.00	0.0925
KCA Jun LD Shallow ASW	46.76	8.46	0.00	0.1020
KCA Jun HD ASUW	55.98	30.19	0.05	0.1450
KCA Jun LD ASUW	43.62	17.20	0.04	0.1090
SOJ Jun HD Deep ASW	17.50	2.86	0.00	0.0616
SOJ Jun LD Deep ASW	18.91	3.03	0.00	0.0623
SOJ Jun HD Shallow ASW	11.63	1.20	0.00	0.0509
SOJ Jun HD ASUW	2.43	0.47	0.00	0.0396
SOJ Jun LD ASUW	1.43	0.34	0.00	0.0382
ECS Oct HD Deep ASW	8.11	0.42	0.00	0.0472
ECS Oct LD Deep ASW	11.83	1.09	0.00	0.0520
ECS Oct HD Shallow ASW	15.36	4.71	0.00	0.0611
ECS Oct HD ASUW	49.23	13.99	0.00	0.1100
ECS Oct LD ASUW	51.90	25.39	0.99	0.1420
KCA Oct HD Deep ASW	35.68	4.53	0.00	0.0861
KCA Oct LD Deep ASW	33.48	3.38	0.00	0.0834
KCA Oct HD Shallow ASW	50.74	8.34	0.00	0.1060
KCA Oct HD ASUW	43.63	8.51	0.02	0.0997
KCA Oct LD ASUW	47.49	6.93	0.07	0.1030
SOJ Oct HD Deep ASW	29.61	5.11	0.00	0.0793
SOJ Oct LD Deep ASW	26.55	4.41	0.00	0.0777
SOJ Oct HD Shallow ASW	36.71	8.79	0.00	0.0921
SOJ Oct HD ASUW	91.45	84.11	1.82	0.3030
SOJ Oct LD AUW	81.77	62.30	1.01	0.2410

tactic depth band (Table II). In other words, one or both ASUW tactics tended to have the highest probability values followed by the shallow ASW tactic, with the deep ASW tactics having the lowest probability values. Interestingly, this trend is reversed for the SOJ on June 30, 2001. The other obvious tendency is for the values of μ_1 to be several times greater than the values of μ_2, reiterating the decaying pattern.

The highest μ_1 is 91.5%, attained by the high Doppler ASUW tactic in the SOJ October case. The low Doppler ASUW tactic in the same case also has a high value at 81.8%. The next high values are in the 50% range. The same two scenarios also achieved the highest μ_2, with 84.1% and 62.3%, respectively. The next high values are about 30% or lower. Only nine of the histograms had nonzero μ_3 [i.e., $\mathrm{Prob}(\mathrm{RD} > 0.5)$] values (not shown in Table II), all of them being for ASUW tactics, the largest of which is 1.8%. These scenarios with high probability values are the ones in which the outcome of an engagement will most likely be different because they have a higher chance of having large differences in predicted performance.

The lowest μ_1 is 1.4%, attained by the low Doppler ASUW tactic in the SOJ on June 30, 2001. The high Doppler ASUW tactic in that case also has a very low value of 2.4%. The next lowest is 8.1%, three times more than the minimum probability. The same two scenarios also achieved two of the lowest μ_2, 0.3% and 0.5%, respectively. The high Doppler deep ASW tactic for ECS on October 10, 2001 has the other lowest value of 0.4%. The next lowest values are more than 1%. These scenarios with low probability values are the ones least likely to have had an impact on engagement outcome because they have a very low chance of having large differences in predicted performance.

The mean RDs decreased with tactic depth band (Table II), except for the SOJ on June 30, 2001. This pattern makes sense since scenarios with a higher mean RD would be expected to have a higher probability of having larger relative differences. The highest mean RDs are 0.303 and 0.241, attained again by the high and low Doppler ASUW tactics in the SOJ on October 10, 2001. The next highest are less than 0.15. The lowest mean RDs are 0.0382 and 0.0396, attained again by the low and high Doppler ASUW tactics in the SOJ on June 30, 2001. The next lowest is 0.0472.

For the deeper-based tactics, at least three factors seemed to influence the amount of relative difference in the WAPP output. The first is the peak value of the horizontal rmsd of the MODAS SSP, which causes high values of the mean RD, μ_1 and μ_2. The second factor is the depth of this peak. A deeper depth of the rmsd peak leads to higher WAPP output values. Finally, the shape of the peak played a partial role, as the higher values can also be associated with broader peaks vice narrower ones. The cases with the obviously larger values in Table II, which shows WAPP output values for both of the deep ASW tactics, are the SOJ on October 10, 2001 and the KCA on June 30 and October

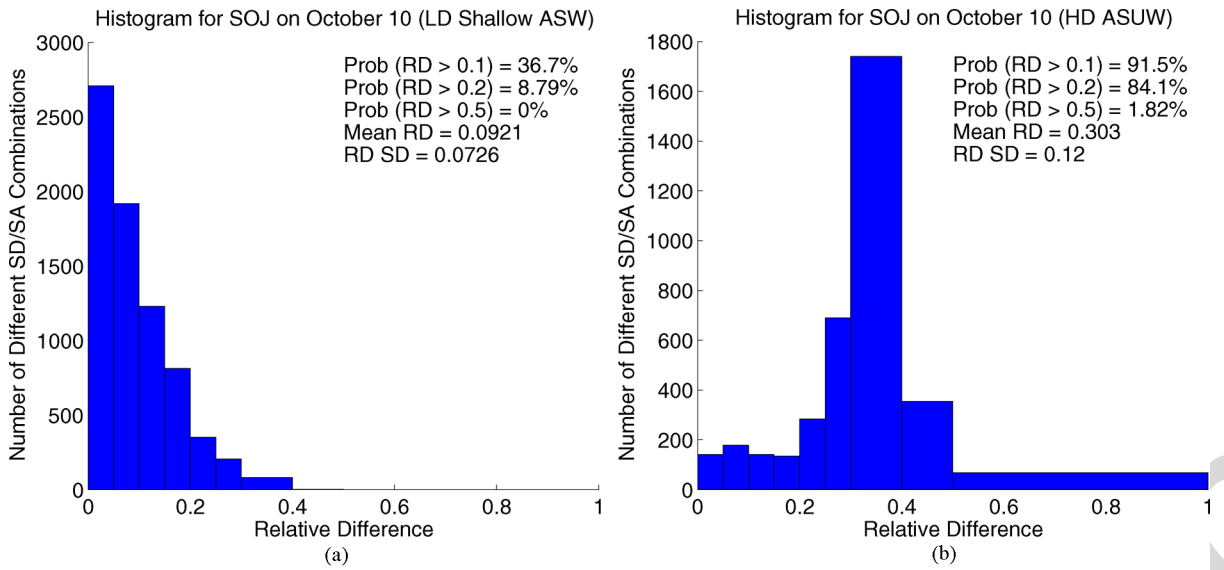

Fig. 15. Histogram of RD of weapon acoustic presets in SOJ for the (a) low Doppler shallow ASW and the (b) high Doppler ASUW.

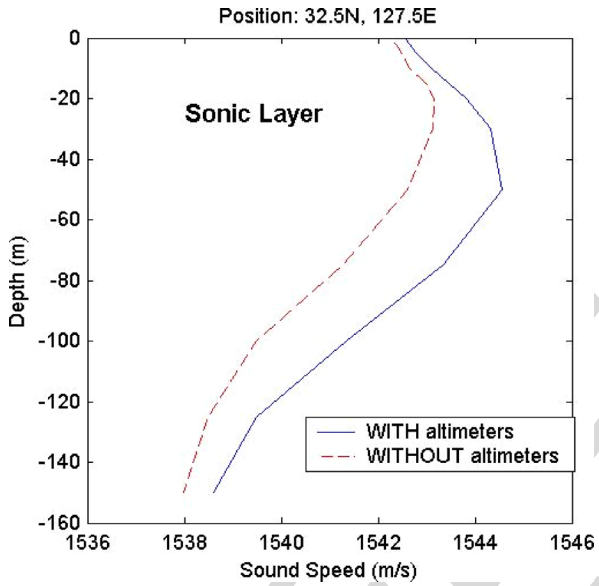

Fig. 16. Comparison of MODAS SSP at 32.5° N, 127.5° E on October 10, 2001 with and without satellite altimetry data assimilated. Note the existence of a sonic layer.

10, 2001 (the same is true for the shallow ASW tactic). All three of these have one or more of the aforementioned factors in their favor.

These results can be understood using Fig. 4, the horizontal rmsd for KCA on October 10, 2001, which shows 2-m/s or larger values occurring in a band from about 100 to 700 m. This band encompasses much of the depth zones of interest for both the deep and shallow ASW tactics (down to about 400 and 200 m, respectively). The MODAS SSPs in Fig. 10 further illustrate the large differences in SSP at these depths. The larger these differences (higher the rmsd peak value) are and the more they extend into the depth zone of interest (owing to the depth and shape of the peak), the larger the difference in the predicted sound propagation for the two MODAS fields in that depth zone is, thus leading to the large probability and mean RD values in WAPP's output for the ASW tactics.

VIII. Overall Sensitivity

From the preceding discussion it is apparent that, in some of the scenarios, WAPP output was quite sensitive to changes in input environmental fields, such as MODAS with satellite altimetry data assimilated versus MODAS without altimetry data. Table II also shows a compilation of the probability values for each scenario, grouped by case, in an effort to more easily compare the sensitivities of each scenario. The μ_1 values range from 1.4 to 91.5 and the μ_2 values range from 0.3 to 84.1, which suggest that the sensitivity of WAPP is extremely variable and, therefore, so is the chance of affecting the outcome of an engagement. Although the ranges are large, most of the 30 scenarios are in the lower halves of them; only one sixth has μ_1 values greater than 50%, one third has values greater than 40%, just over half has values greater than 30%, and only one tenth of the scenarios has μ_2 values greater than 30%. Based on this sensitivity analysis, the satellite altimetry data contributed as much as an 80%–90% chance of having a different engagement outcome (once again, assuming 0.1–0.2 is enough of a relative difference in area coverage to change the outcome), but in most of the scenarios the contribution is less than 50%.

IX. Physical Mechanisms

A. Sonic Layer

A sonic layer occurs when the sound speed increases with depth from the surface to a maximum and then decreases with depth (Fig. 16). A stronger sonic layer would have two effects on near-surface sound-propagation characteristics. If the sound source were in the layer, it would more effectively trap the sound energy by refracting it back to the surface, where it would be reflected back into the water, allowing it to travel greater distances before being diminished. For a source below the layer, it would more effectively prevent sound energy from penetrating

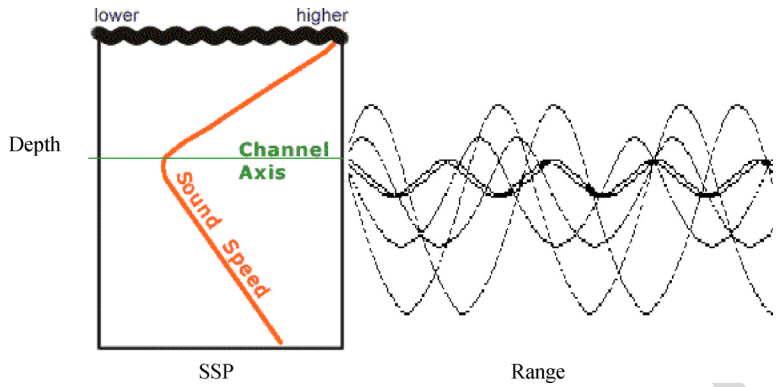

Fig. 17. Sound channel depiction.

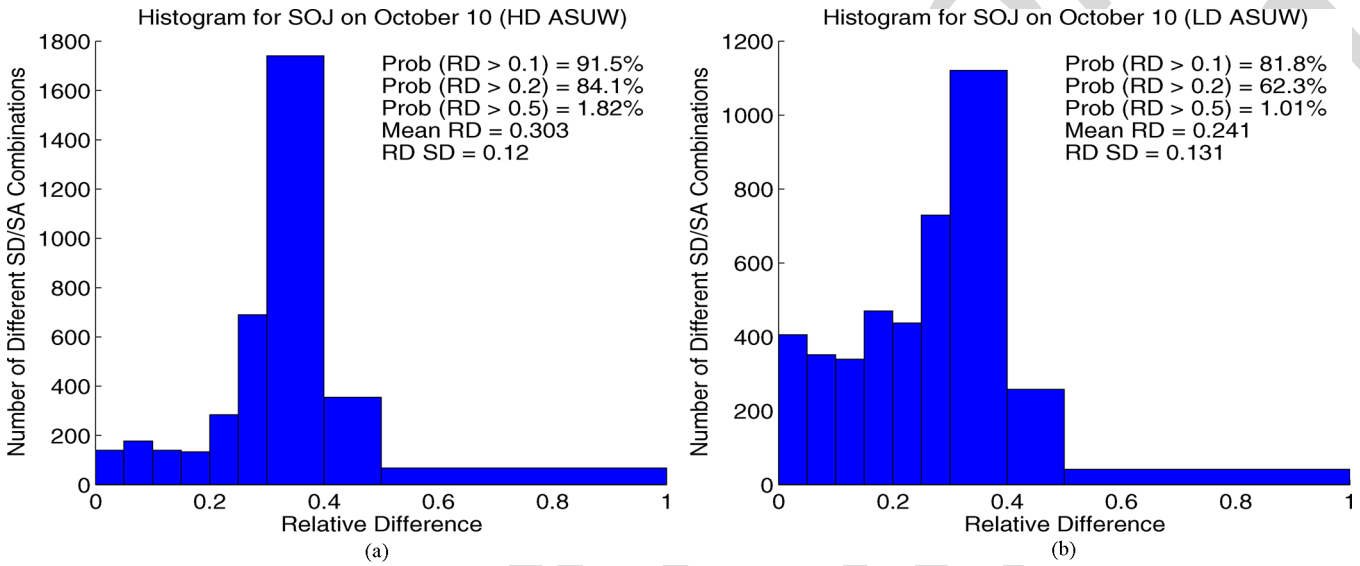

Fig. 18. Histogram of RD of weapon acoustic presets in SOJ for (a) high Doppler shallow ASW and (b) low Doppler ASUW on October 10, 2001.

into it by refracting it down away from the layer, creating a relatively sound-free layer near the surface. Because only one of the MODAS fields produced these effects in each case, the sound-propagation characteristics near the surface would differ substantially resulting in equally dissimilar predictions of sound propagation. This is what led to more significant differences in the presets that WAPP produced for the shallower-based tactics.

B. Sound Channel

One reason for the differences in the ASW scenarios is the existence of sound channels. Sound channels exist when sound speed first decreases with depth and then increases again (see Fig. 17). This produces a refractive environment that focuses the sound energy in a depth band about the channel axis, due to bending above and below the axis. This focusing allows the sound to be detectable at longer distances than it otherwise would because it is less spread out and, thus, more intense. When a sound channel exists or is stronger in one MODAS field, the channeling effect produces significant differences in sound propagation between the two fields.

C. Two Extreme Cases

The two cases with the largest relative differences in WAPP area coverage for ASUW and ASW tactics deserve a closer look: the SOJ on October 10, 2001 for the ASUW tactics and the KCA on June 30, 2001 for the ASW tactics. The former case is examined in detail during the MODAS discussion. Recall that rmsds greater than 3 °C existed in a band from 50 to 200 m due to both a subsurface eddy system and a stronger SOJ polar front. These produced large differences in the SSPs in this depth band (Fig. 11) and associated large horizontal rmsd temperature [Fig. 4(b)]. This shows a very pronounced sonic layer over much of the SOJ region in the MODAS field with satellite altimetry data, but almost no such layer in the MODAS field without satellite altimetry data.

As discussed earlier, the effect of the sonic layer would be to cause WAPP to generate very different near-surface sound-propagation predictions for the two MODAS fields, leading to the large relative differences in area coverage. In the histograms for the two ASUW tactics, shown in Fig. 18, the radically displaced relative difference peaks (in the bin for 0.3–0.4) as compared to the rest of the histograms are apparent. Once again, these two scenarios had the highest probability values and mean

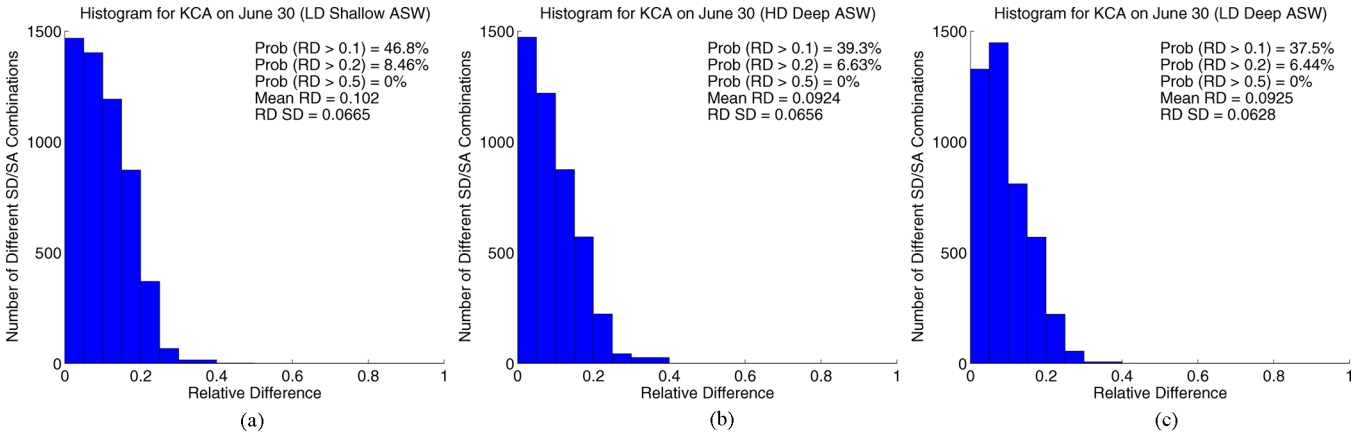

Fig. 19. Histogram of RD of weapon acoustic presets in SOJ for (a) high Doppler shallow ASW, (b) low Doppler deep ASW, and (c) high Doppler deep ASW on June 30, 2001.

RDs of all the scenarios, not just the ASUW ones, and so were very likely to have a different outcome in an actual engagement.

The much larger differences seem to be due to the extra large differences in the MODAS fields. Fig. 11 shows that the sonic layer in the altimetry field is very strong, with sound speed increasing by several meters per second over the depth of the layer in several locations. Some of the other scenarios have equally strong sonic layers, but only in one or two locations. The other big difference that sets these two scenarios apart from the rest is that the other MODAS field (nonaltimetry, in this case) had no appreciable sonic layer anywhere in the region. The other scenarios with strong sonic layers in one field also have a weaker sonic layer in the other field, which helps to offset the difference and apparently limit the effect on WAPP's output.

Shifting now to the largest WAPP output differences for ASW tactics, the KCA on June 30, 2001 just edge out that on October 10, 2001 in the same region***[AU: this sentence is unclear. Please rewrite]***. These two cases have very similar MODAS fields, as discussed in Section VI, and they are both mentioned earlier as having all three influencing factors in their favor: a high sound-speed rmsd peak value, a peak axis well into the depth zone of interest, and a broad peak increasing the extent of the high rmsd values throughout most of the zone of interest.

As discussed for the general case, this depth zone includes most of the ASW zone of interest. Therefore, the predicted sound propagation for the two MODAS fields in the ASW zone was more dissimilar, thus leading to the large differences in WAPP's output for the ASW tactics.

The large differences in the sound-speed fields in the ASW depth zone of interest are partially due to the MODAS field with altimetry having a stronger sound channel, evident in the top-right two panels, which are produced by the stronger frontal gradients in that MODAS field for June 30, 2001 (Fig. 14) and October 10, 2001 (Fig. 10). Another contribution to the sound-speed differences in the ASW band can be seen in the four bottom-left panels, which show a second sound channel with an axis near 100 m in the altimetry field profiles, where one does not exist (or is very weak) in the nonaltimetry field. As discussed earlier, these sound channels would refract sound in a way that would significantly affect sound propagation and, therefore, the output of WAPP when using this MODAS field. The outcome of an engagement would probably have been significantly different, depending on which MODAS field was used. For completeness, the histograms for the three ASW tactics are shown in Fig. 19.

X. Conclusion and Recommendations

The scenarios in which WAPP is the most sensitive are the ones where the input MODAS fields differed significantly, especially in the depth zone of interest for the given tactic. The MODAS fields usually differed in their depiction of mesoscale features, such as eddy systems (e.g., in SOJ on October 10, 2001) and subsurface fronts (e.g., in KCA on June 30 and October 10, 2001), due to only one field having the benefit of satellite altimetry data to help MODAS resolve them. This causes differences in the SSP characteristics for the two fields, such as the sonic layer being more pronounced, sound channels being stronger and, in some cases, one of the fields having no sonic layer or having secondary sound channels. Quite expectably, this led to large differences in the sound-propagation predictions made by WAPP for the two fields, and thus to large relative differences in area coverage.

The most accurate way to assess the satellite altimetry data's overall value is to relate it to how it would affect the outcome of an actual engagement, or weapon effectiveness. The value could then be based on whether the outcomes were affected positively, which in an ASW engagement typically means the torpedo hit the target versus missed it. In this paper, torpedo performance in the real world is not readily quantifiable because, although the MODAS field with satellite altimetry is certainly closer to the actual environmental conditions, neither field can be considered as being the actual environment like an *in situ* measurement can (within the accuracy of the device used). Therefore, there is no way to relate the performance predictions to the expected real-world performance. (The only real-world performance assertion is made to single out the different SD/SA combinations for the sensitivity analysis, namely that the engagement will be very similar if the weapon is assigned the same presets, regardless of which MODAS field is used). Also, a relative difference in area coverage of 0.1 to 0.2 was arbitrarily chosen for analysis,

although higher or lower levels of difference may actually be necessary to affect engagement outcome.

To quantify the effect on weapon effectiveness, a two-part study needs to be conducted. Part 1 compares the output of WAPP using MODAS fields (one with altimetry data and one without, as done here) and *in situ* measurements of the local environment. The *in situ* measurements can be performed by any number of assets, such as a U.S. Navy ship during an exercise or a research vessel, although the area should be one with large variability, such as in the Gulf Stream or Kuroshio Current, to obtain the most benefit from the altimetry data. Of course, as with any experiment involving *in situ* measurements, the data set will be much smaller than the one used in this study.

With this type of comparison, any differences in WAPP output could be correlated to the torpedo's predicted real-world performance and, therefore, so could the benefit of the satellite altimetry data. For example, if the predicted performance is similar for the MODAS field with altimetry and the *in situ* data, but the performance differed appreciably for the MODAS field without altimetry, the altimetry data would be quite valuable. If the predicted performance differed appreciably between all three inputs or between the *in situ* input and both MODAS fields, the altimetry data would be deemed as being less beneficial. However, the predicted performance is still not a real-world performance.

To assess the effect of the satellite altimetry data on weapon effectiveness even better, part 2 needs to include simulations of torpedo engagements. The Weapons Analysis Facility at NUWC, Division Newport has the capability to simulate engagements using torpedo hardware-in-the-loop and a high-fidelity virtual environment. Using the Weapon Analysis Facility and presets generated by the MODAS fields and the *in situ* data in part 1, many virtual torpedo engagements can be conducted to examine the effects of the different MODAS fields on virtual performance. This can be done for any number of scenarios, by alternately using presets generated by each of the environmental inputs to WAPP: the MODAS field without altimetry, the MODAS field with altimetry, and the *in situ* data; and then, comparing the ratios of hits to misses for the virtual engagements.

This experiment introduces an operational element by enabling the presets to be chosen by an operator for each engagement. It also eliminates the need to use the relative difference in area coverage and the associated uncertainty in the threshold that produces changes in engagement outcome. This is because the proposed metric, the hit–miss ratio, is not a prediction of performance (like area coverage) but, rather, a direct assessment of it (once again, in a virtual environment). Aside from the cost and logistics prohibitive alternative of putting many torpedoes in the water, an experiment such as this would provide the next best analysis of the value of assimilating satellite altimetry data into MODAS with regard to torpedo effectiveness.

Finally, to arrive at answers to some of the broader questions in this line of research, other comparisons need to be included. These are the questions of how many satellite altimeters are required to ensure maximum weapon effectiveness and at what point additional altimeter input no longer increases weapon effectiveness. To answer these questions, MODAS fields with varying number of altimeters assimilated would need to be used as environmental inputs to WAPP and could be incorporated into part 1 or added at a later date.

REFERENCES

[1] M. R. Carnes, D. Fox, and R. Rhodes, "Data assimilation in a north Pacific ocean monitoring and prediction system," in *Modern Approach to Data Assimilation in Ocean Modeling*, P. Malanote-Rizzoli, Ed. New York: Elsevier, 1996, pp. 319–345.

[2] M. R. Carnes, L. Mitchell, and P. W. deWitt, "Synthetic temperature profiles derived from Geosat altimetry: Comparison with air-dropped expendable bathythermograph profiles," *J. Geophys. Res.*, vol. 95, no. C10, pp. 17 979–17 992, 1990.

[3] C. T. Chen and F. J. Millero, "Speed of sound in seawater at high pressures," *J. Acoust. Soc. Amer.*, vol. 62, pp. 1129–1135, 1977.

[4] P. C. Chu, M. D. Perry, E. L. Gottshall, and D. S. Cwalina, "Satellite data assimilation for improvement of naval undersea capability," *Marine Technol. Soc. J.*, vol. 38, no. 1, pp. 11–23, 2004.

[5] P. C. Chu, W. Guihua, and C. Fan, "Evaluation of the U. S. Navy's modular ocean data assimilation system (MODAS) using south china sea monsoon experiment (SCSMEX) data," *J. Oceanography*, vol. 60, pp. 1007–1021, 2004.

[6] P. C. Etter, *Underwater Acoustic Modeling: Principles, Techniques and Applications*. New York: Elsevier, 1991, p. 305.

[7] D. N. Fox, W. J. Teague, C. N. Barron, M. R. Carnes, and C. M. Lee, "The modular ocean data assimilation system (MODAS)," *J. Atmos. Ocean. Technol.*, vol. 19, pp. 240–252, 2002.

[8] D. N. Fox, C. N. Barron, M. R. Carnes, M. Booda, G. Peggion, and J. Gurley, "The modular ocean data assimilation system," *Oceanography*, vol. 15, pp. 22–28, 2002.

[9] R. E. Francois and G. R. Garrison, "Sound absorption based on ocean measurements. Part 1: Pure water and magnesium sulfate contribution," *J. Acoust. Soc. Amer.*, vol. 72, pp. 896–907, 1982.

[10] ——, "Sound absorption based on ocean measurements. Part 2: Boric acid contribution and equation for total absorption," *J. Acoust. Soc. Amer.*, vol. 72, pp. 1879–1890, 1982.

[11] ***[AU: Please provide department]***S. Mancini, "Sensitivity of satellite altimetry data assimilation on a naval anti-submarine weapon system," M. S. thesis, Naval Postgraduate School, Monterey, CA, 2004.

[12] H. Medwin and C. S. Clay, *Fundamentals of Acoustic Oceanography*. New York: Academic, 1997, p. 712.

[13] P. J. Washburn, "MODAS – The warfighters' view of the undersea environment," *NMOC News*, vol. 24, p. 2, 2004.

Peter C. Chu received the Ph.D. degree in geophysical fluid dynamics from the University of Chicago, Chicago, IL, in 1985.

He is a Professor of Oceanography and Head of the Naval Ocean Analysis and Prediction (NOAP) Laboratory, the Naval Postgraduate School, Monterey, CA. His research interests include ocean analysis and prediction, coastal modeling, littoral zone oceanography for mine warfare, mine-impact burial prediction, mine acoustic detection, and satellite data assimilation for undersea warfare.

Steven Mancini was born in Cincinnatti, OH, on April 21, 1971. He received the B.S. degree in applied physics from Xavier University, Cincinnatti, OH, in 1992 and the M.S. degree in meteorology and physical oceanography from the Naval Postgraduate School, Monterey, CA, in 2004.

Since November 2004, he has been present METOC/Asst. Surf. Ops/Scheduler ***[AU: Please define "METOC" and spell out the title]*** at the Commander Carrier Group Seven, North Island, CA. From June 1992 to September 1992, he was a Student at the Officer Candidate School, Newport, RI. From October 1992 to April 1993, he was a Student at the Naval Nuclear Power School, Orlando, FL. From May 1993 to November 1993, he was a student at the NPTU Idaho Falls, ID. From December 1993 to May 1994, he was a Student at the Surface Warfare Officer School, Newport, RI. From June 1994 to June 1996, he was with the Reactor Department, U.S.S. Enterprise (CVN 65), Norfolk, VA. From July 1996 to September 1997, he was with the Combat Systems Department, U.S.S. Saipan (LHA 2), Norfolk,

VA. From October 1997 to September 1999, he was with the C4I Department, Commander Operational Test and Evaluation Force, Norfolk, VA. From October 1999 to December 1999, he was a Student at the Basic Oceanography Accession Training, Gulfport, MS. From January 2000 to June 2002, he was with the Operations Department, Naval Pacific Meteorology and Oceanography Center, San Diego, CA. From July 2002 to October 2004, he was a Student at the Naval Postgraduate School, Monterey CA.

Eric L. Gottshall received advanced degrees in physics and meteorology and physical pceanography.***[AU: what degrees, in what year and from what university?]***

He is an Active Duty Navy Oceanographer currently assigned as an Associate Director for Ocean, Atmosphere, and Space Sciences at the Office of Naval Research Global, London, U.K. ***[AU: This affiliation does not match the one on p.1. Please advise.]***He is the Defense Acquisition Workforce Level III certified in systems planning, research, development, and engineering. He is a member of the Navy's Space Cadre

David S. Cwalina was born in Peabody, MA, on November 9, 1957. He received the B.S. degree in physics from the University of Massachusetts, Lowell, in 1979, the M.S. degree in computer and systems engineering from Rensselaer Polytechnic Institute, Troy, NY, in 1982, and the M.S. degree in electrical engineering from the University of Rhode Island, Kingston, in 1992.

In 1982, he joined the Naval Underwater Systems Center (now Naval Undersea Warfare Center) in the Combat Control Systems Department. Currently, he works in the areas of torpedo and unmanned vehicle engagement planning, modeling and simulation, guidance and control, and performance prediction.

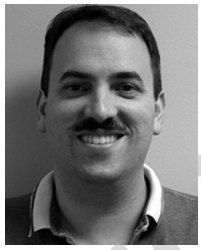

Charlie N. Barron received the Ph.D. degree in oceanography from Texas A&M University***[AU: Location?]*** in 1994.

He is an oceanographer at the U.S. Naval Research Laboratory, Stennis Space Center, MI, specializing in global ocean modeling and data assimilation.

Peer-Reviewed Technical Communication

Sensitivity of Satellite Altimetry Data Assimilation on a Weapon Acoustic Preset

Peter C. Chu, Steven Mancini, Eric L. Gottshall, David S. Cwalina, and Charlie N. Barron

***Abstract*—The purpose of this research is to assess the benefit of assimilating satellite altimeter data for naval undersea warfare. To accomplish this, sensitivity of the weapon acoustic preset program (WAPP) for the Mk 48 variant torpedo to changes in the sound-speed profile (SSP) is analyzed with SSP derived from the modular ocean data assimilation system (MODAS). The MODAS fields differ in that one uses altimeter data assimilated from three satellites while the other uses no altimeter data. The metric used to compare the two sets of outputs is the relative difference in acoustic coverage area generated by WAPP. Output presets are created for five different scenarios, two antisurface warfare scenarios, and three antisubmarine warfare scenarios, in each of three regions: the East China Sea, Sea of Japan, and an area south of Japan that includes the Kuroshio currents. Analysis of the output reveals that, in some situations, WAPP output is very sensitive to the inclusion of the altimeter data because of the resulting differences in the subsurface predictions. The change in weapon presets can be so large that the effectiveness of the weapon may be affected.**

***Index Terms*—Antisubmarine warfare, antisurface warfare, modular ocean data assimilation system (MODAS), satellite altimetry data, weapon acoustic preset.**

I. Introduction

THE outcome of a battlefield engagement is often determined by the advantages and disadvantages held by each adversary. On the modern battlefield, the possessor of the best technology often has the upper hand, but only if that advanced technology is used properly and efficiently. To exploit this advantage and optimize the effectiveness of high-technology sensor and weapon systems, it is essential to understand the impact on them by the environment. In the arena of antisubmarine warfare (ASW), the ocean environment determines the performance of the acoustic sensors employed and the success of any associated weapon systems. Since acoustic sensors detect underwater sound waves, understanding how those waves propagate is crucial to knowing how the sensors will perform and being able to optimize their performance in a given situation. To gain this understanding, an accurate depiction of the ocean environment is necessary.

How acoustic waves propagate from one location to another under water is determined by many factors, some of which are described by the sound-speed profile (SSP). If the environmental properties of temperature and salinity are known over the entire depth range, the SSP can be estimated by using them in an empirical formula to calculate the expected sound speed in a vertical column of water. One way to determine these environmental properties is to measure them *in situ*, such as by conductivity–temperature–depth (CTD) or expendable bathythermograph (XBT) casts. This method is not always tactically feasible in the ASW scenario since the release of XBT will catch enemy's attention. Another method is to estimate the ocean conditions using a computer analysis tool, such as the modular ocean data assimilation system (MODAS) developed by the Naval Research Laboratory, Stennis Space Center, MI. MODAS assimilates *in situ* measurements such as XBT and remotely sensed data from satellites such as sea surface temperature (SST) from radiometers and sea surface height (SSH) from radar altimeters. MODAS represents real-time ocean thermohaline structure better than static climatology databases such as the U.S. Navy's generalized digital environmental model (GDEM) [7], [8], [4], and can improve the weapon acoustic weapon presets [5]. If MODAS provides an improved representation of actual ocean conditions when satellite altimetry data is assimilated, a MODAS field that has this information will differ from one that does not, especially in regions of high mesoscale activity. If these differences are large enough, a tactical decision aid may give very different sound-propagation characteristics depending on which MODAS field is used to represent the ocean environment. This, in turn, would cast doubt on predicted sensor performance and could render the technology ineffective, possibly changing the outcome of an engagement.

The purpose of this paper is to quantify the sensitivity of a naval ASW system, specifically the Mk 48 torpedo WAPP, to the assimilation of satellite altimetry data when MODAS is used as WAPP's source of SSP information. Since inclusion of SSH data is not always closely tied to relevant changes in SSP for weapon systems, and since it does not always represent an improvement in the predicted SSP, a convenient operational model MODAS is used to develop alternative SSPs and to validate the WAPP design and implementation. This is done by examining the relative difference (RD) in the output of WAPP when two

Manuscript received September 23, 2004; accepted January 4, 2006. This work was supported in part by the Space and Naval Warfare System Command, the Naval Undersea Warfare Center, Newport, RI, the Naval Research Laboratory, and the Naval Postgraduate School.

Associate Editor: L. Goodman.

P. C. Chu and S. Mancini are with the Naval Ocean Analysis and Prediction Laboratory, Department of Oceanography, Naval Postgraduate School, Monterey, CA 93943 USA (e-mail: pchu@nps.edu).

E. L. Gottshall is with the Space and Naval Warfare System Command, San Diego, CA 92110 USA.

D. S. Cwalina is with the Combat Control Systems Department, Naval Undersea Warfare Center, Newport, RI 02841 USA.

C. N. Barron is with the Naval Research Laboratory, Stennis Space Center, MI 39529 USA.

Color versions of one or more of the figures in this paper are available online at http://ieeexplore.ieee.org.

Digital Object Identifier 10.1109/JOE.2006.888869

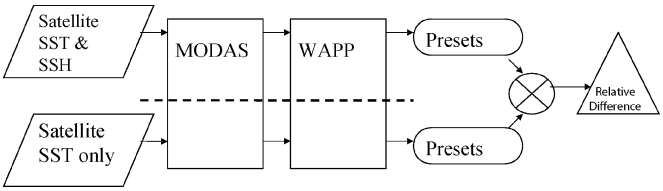

Fig. 1. Flow chart of the sensitivity study. Two MODAS SSP data sets with and without satellite altimeters are used for WAPP to generate two sets of weapon acoustic preset. Computing the relative difference between the two preset data sets gives the sensitivity of using satellite altimeters.

different MODAS fields are used as separate SSP inputs, as depicted in Fig. 1. The MODAS fields were identical in each case except that one has satellite altimetry data assimilated while the other does not [11].

If a significant degree of sensitivity is discovered, then the next logical step is to determine if the addition of satellite altimetry causes WAPP to respond more like it would have if *in situ* measurements were used as SSP input. This can be achieved in an experiment designed to compare WAPP output when MODAS fields and *in situ* measurements are used as separate SSP inputs. The question of how valuable this altimetry data is can then be more fully explored. On the other hand, if this paper shows little sensitivity to the different MODAS fields, then the value of satellite altimetry information, at least as an input to MODAS, can be assessed as low. Thus, this paper describes the WAPP validation. MODAS will strive to achieve the best SSP set possible because the variability of profiles and the sensitivity thresholds of other users have already demonstrated the need to consider SSH data, where appropriate.

II. MODAS

MODAS is one of the present U.S. Navy standard tools for production of 3-D grids of temperature and salinity. It is a modular system for ocean analysis and is built from a series of formula translator (FORTRAN) programs and Unix scripts that can be combined to perform desired tasks [5]. MODAS was designed to combine observed ocean data with climatological information to produce a quality-controlled, gridded analysis field as an output. The analysis uses an optimal interpolation (OI) data assimilation technique to combine various sources of data [7], [8], [13].

A. Static and Dynamic MODAS

MODAS has two modes of usage: static and dynamic MODAS. Static MODAS climatology is an internal climatology used as MODAS' first guess field. The other mode is referred to as the dynamic MODAS, which combines locally observed and remote sensed ocean data with climatological information to produce a near-real-time gridded 3-D analysis field of the ocean temperature and salinity structure as an output. Grids of MODAS climatological statistics range from 30-min resolution in the open ocean to 15-min resolution in shallow waters and 7.5-min resolution near the coasts in shallow water regions.

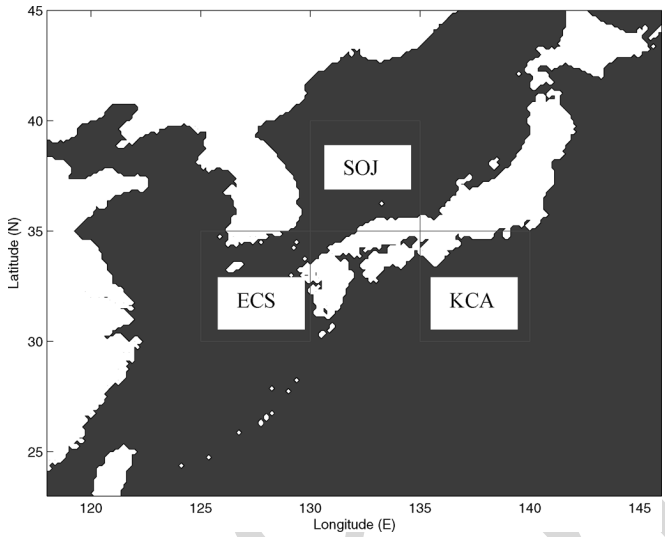

Fig. 2. Geographic regions selected for the study.

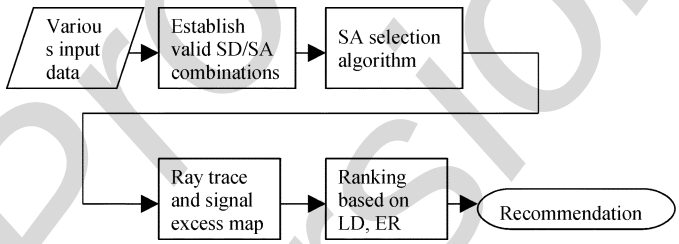

Fig. 3. Flow chart for illustrating the WAPP presetting procedure.

B. Synthetic Temperature and Salinity Profiles

Traditional oceanographic observations, such as CTD, XBT, etc., are quite sparse and irregularly distributed in time and space. It becomes important to use satellite data in MODAS for establishing real-time 3-D T/S ***[AU: Please define "T/S"]*** fields. Satellite altimetry and SST provide global data sets useful for studying ocean dynamics and for ocean prediction. MODAS has a component for creating synthetic temperature and salinity profiles [2], [1], which are the functions of parameters measured at the ocean surface such as satellite SST and SSH. These relationships were constructed using a least square regression analysis performed on archived historical database of temperature and salinity profiles (e.g., MOODS).

The following three steps are used to establish regression relationships between the synthetic profiles and satellite SST and SSH: 1) computing regional empirical orthogonal functions (EOFs) from the historical temperature and salinity profiles, 2) expressing the T/S profiles in terms of EOF series expansion, and 3) performing regression analysis on the profile amplitudes for each mode with the compactness of the EOF representation allowing the series to be truncated after only three terms while still retaining typically over 95% of the original variance [1].

C. First Guess Fields

The MODAS SST field uses the analysis from previous days field as the first guess, while the MODAS' 2-D SSH field uses a large scale weighted average of 35 d of altimeter data as a first

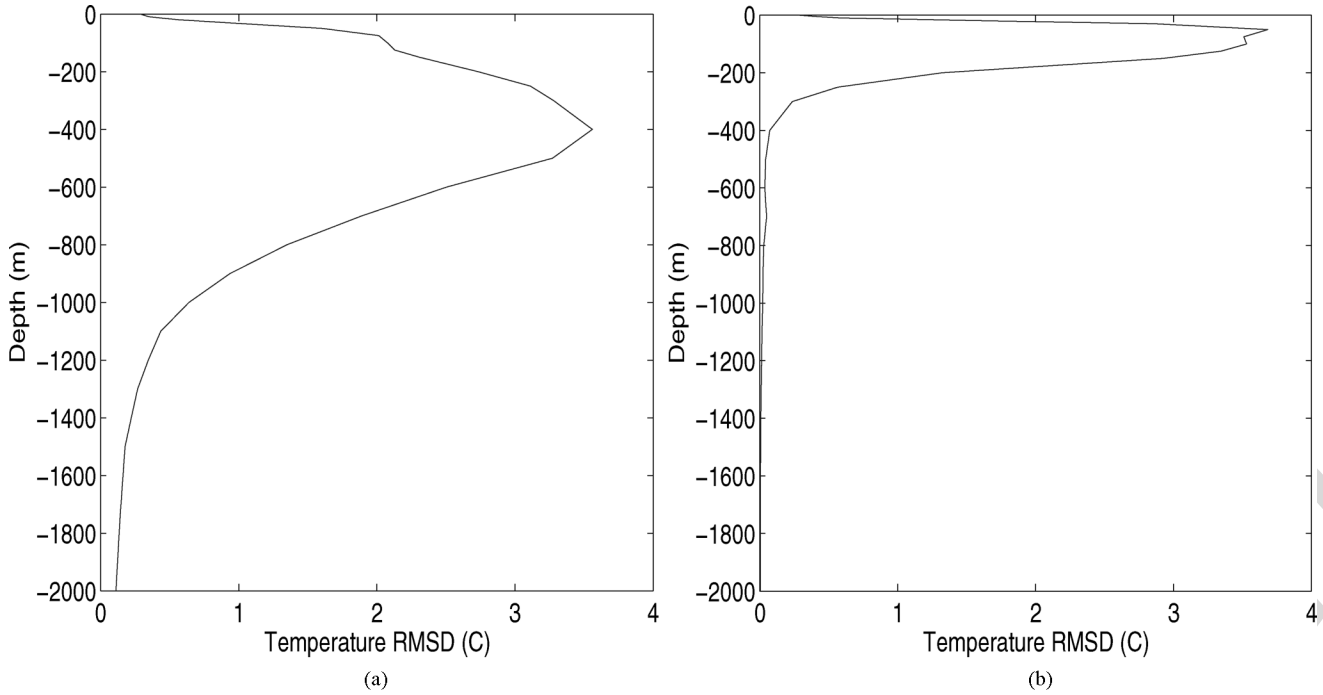

Fig. 4. Horizontal rmsd of MODAS temperature for (a) KCA and (b) SOJ on October 10, 2001.

TABLE I
VOLUME RMSD OF THE SIX MODAS FIELD PAIRS FOR SOUND SPEED (METER PER SECOND), TEMPERATURE (CELSIUS DEGREES), AND SALINITY (PRACTICAL SALINITY UNIT) IN 2001

	T (°C)	S (psu)	Sound Speed (m/s)
ECS Jun 30	1.12	0.81	1.12
KCA Jun 30	1.59	0.78	1.61
SOJ Jun 30	1.19	0.43	1.17
ECS Oct 10	1.04	0.58	1.16
KCA Oct 10	1.80	0.81	1.82
SOJ Oct 10	1.78	0.43	1.64

guess. The deviations calculated from the first guess field and the new observations are interpolated to produce a field of deviations from the first guess. Next, a final 2-D analysis is calculated by adding the field of deviations to the first guess field. When the model performs an optimum interpolation for the first time it uses the static MODAS climatology for the SST first guess field and zero for the SSH first guess field. Every day after the first optimum interpolation it uses previous day's first guess field for SST and a large scale weighted average is used for SSH. Synthetic profiles are generated at each location based on the last observation made at that location. If the remotely obtained SST and SSH for a location do not differ from the climatological data for that location, then climatology is used for that profile. If the remotely obtained SST and SSH for a location differ from the climatological data for that location then the deviation at each depth are estimated. Adding these estimated deviations to the climatology produces the synthetic profiles.

D. MODAS Fields With and Without Satellite Altimetry Data

Global MODAS fields are produced at the Naval Research Laboratory on a daily basis. The daily MODAS fields chosen for analysis are June 30, 2001 and October 10, 2001. For each day, there are two fields: one with altimetry data assimilated into it and one without altimetry data. The fields that included altimetry received the data from the three satellite systems having operational altimeters at the time: the National Aeronautics and Space Association (NASA's) TOPEX, the U.S. Navy's GEOSAT follow-on, and the European Space Agency's ERS-2 ***[AU: Please define "TOPEX", "GEOSAT" and "ERS"]***. To keep the data analysis manageable, but at the same time to gather a large enough number of data comparison points, three geographic regions, each five-by-five degrees in latitude and longitude, were cut out of the MODAS fields for each day. The boxes, shown in Fig. 2, are located in the East China Sea region (ECS, 30°–35° N, 125°–130° E), the Sea of Japan region (SOJ, 35°–40° N, 130°–135° E), and the Kuroshio Current area south of Japan (KCA, 30°–35° N and 135°–140° E), and are chosen for their varying amounts of mesoscale variability as well as their tactical significance. Segregating these regions by the two dates created six MODAS cases to analyze. These MODAS (T/S) fields are taken as input for the acoustic ray tracing model in the Weapon Acoustic Preset Program (WAPP) to determine suggested presets for a Mk 48 variant torpedo.

The resolution of MODAS in these regions is one eighth of a degree, which yielded three grids of 41-by-41 points each. After eliminating grid points over areas of land, the number of vertical profiles made available to WAPP for each case is as follows: 1495 pairs for SOJ,; 1448 pairs for ECS, and 1436 pairs for KCA, for a total of 4379 pairs of profiles. Each vertical profile pair is for the same location and day, but each is taken from the two different versions of MODAS fields. The output of WAPP can, therefore, be compared using each pair of vertical profiles to determine the sensitivity of the output to the altimetry data.

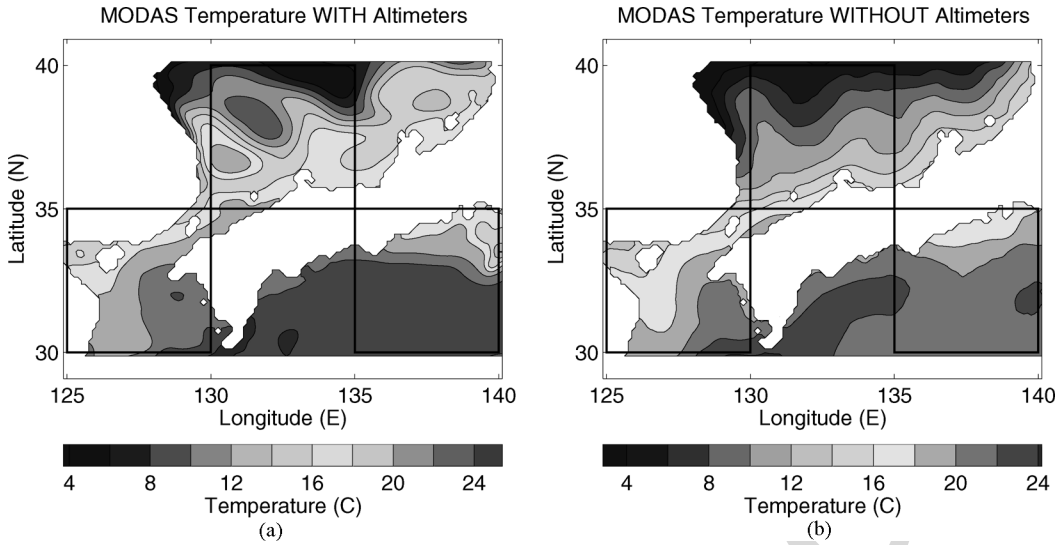

Fig. 5. Comparison between MODAS temperature at 100 m on October 10, 2001 (a) with and (b) without satellite altimetry data assimilated. Here, the upper middle box is used for the SOJ evaluation, the lower right box is used for the KCA evaluation, and lower left box is used for the ECS evaluation (see Fig. 2).

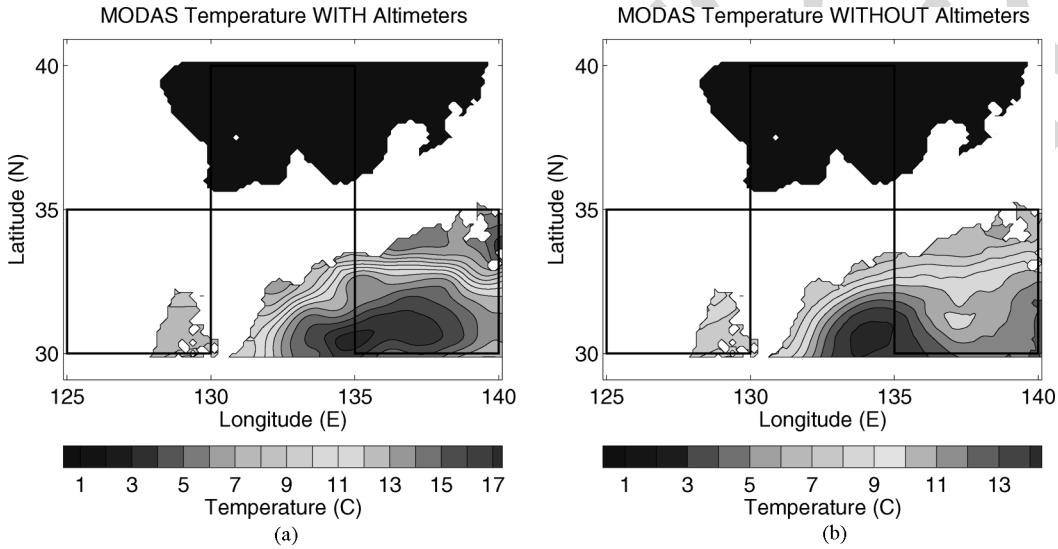

Fig. 6. Comparison between MODAS temperature at 500 m on October 10, 2001 (a) with and (b) without satellite altimetry data assimilated. Here, the upper middle box is used for the SOJ evaluation, the lower right box is used for the KCA evaluation, and lower left box is used for the ECS evaluation (see Fig. 2).

III. WAPP

A. General Description

WAPP is an automated, interactive program designed to provide the fleet with an onboard means of generating acoustic presets for multiple variants of Mk 48 torpedoes and visualizing their performance. Developed by the Naval Undersea Warfare Center (NUWC, Division Newport, RI), it consists of several elements including a graphical user interface (GUI) for entering various data, a computational engine for generating acoustic performance predictions, and various forms of output (NUWC, 2004***[AU: What are you referreing to here?]***).

The types of necessary input data include tactical (such as tactic type and depth zone of interest), target (such as acoustic and Doppler characteristics), weapon (such as type, mod, and active or passive acoustic mode), and environmental information. To input the environmental information, the user selects the "environment" pull-down menu of the GUI to bring up the environmental data entry (EDE) window. This window allows the entry of water-column parameter profiles (such as temperature, salinity, sound speed, and volume scattering strength) for a specified latitude and longitude. Other environmental input entered via the EDE consists of sea surface conditions (wind speed, waveheight, and sea state) and bottom conditions (depth and type). Operationally, the environmental data is received from the sonar tactical decision aid.

B. WAPP Presetting Process

Once the necessary information is input (or default values are selected), WAPP is ready to undergo the presetting process. This process is begun by using the "compute" pull-down menu of the GUI and is outlined in Fig. 3. The first step is to establish a valid set of search depth (SD) and search angle (SA)

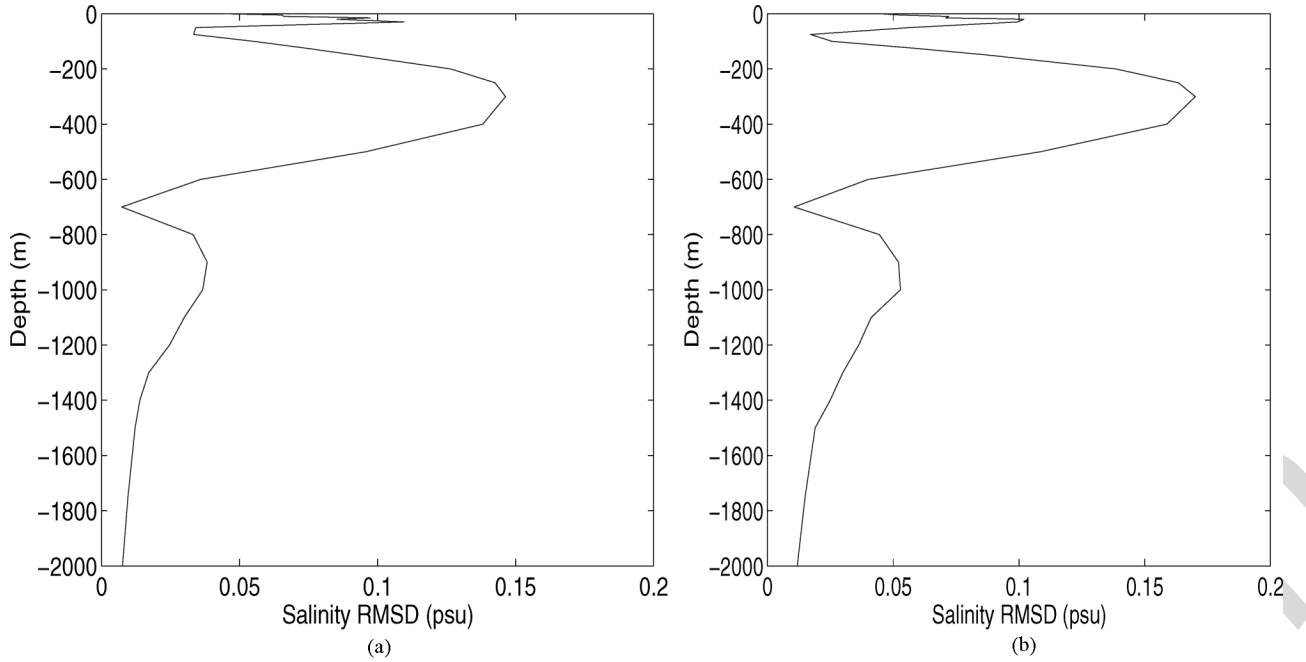

Fig. 7. Horizontal rmsd of MODAS salinity for KCA on (a) June 30, 2001 and (b) October 10, 2001.

combinations. The program then invokes an SA selection algorithm to identify the optimal pitch angle for each SD. Next, the computational engine traces, in a series of time steps, a fan of rays that bound the torpedo beam pattern for each resulting SD/SA combination (NUWC, 2004***[AU: Which reference is this?]***). A signal excess computation is performed and mapped to a gridded search region at each time step using the monostatic, active sonar equation for the reverberation limited case

$$\mathrm{SL} - 2\mathrm{TL} + \mathrm{TS} - \mathrm{RL} - \mathrm{DT} = \mathrm{SE} \tag{1}$$

where

SL	active sonar source level;
TL	two-way transmission loss between the sonar and the target;
TS	target strength;
RL	reverberation level;
DT	detection threshold.

The signal excess map is used to determine the effectiveness ratio (the fraction of the prosecutable search region with signal excess greater than 0 dB, also called area coverage) and laminar distance (the location of signal excess center of mass). Then, WAPP ranks the SD/SA combinations based on these computations (along with some other mitigating factors) and makes a recommendation as to the best preset for the given scenario.

In solving (1), the SL, DT, and TS terms are based on properties of the sonar system and target involved, so they are selected by the program or entered by the user, as is the case for TS. The TL and RL terms are computed using a range-independent, ray theory propagation model that accounts for geometric spreading, refractive effects, volumetric effects, and boundary interactions with the ocean surface and bottom. The vertical SSPs used by the ray tracing model are calculated by WAPP from the temperature and salinity profiles using the equation proposed by Chen and Millero [3]. Geometric spreading and refractive losses are determined using the transmission loss equation derived using ray theory

$$\mathrm{TL} = 10\log\left(\frac{R_k\left|\frac{\partial R_k}{\partial \theta_o}\sin\theta_k\right|}{\cos\theta_o}\right) \tag{2}$$

where R_k is the horizontal range at some position downrange, θ_o is the initial angle of the ray, and θ_k is the angle of the ray at range R_k. Volume absorption is introduced into the transmission loss term using absorption coefficients calculated from the chemical relaxation method proposed by Francois and Garrison [9], [10].

C. Ranked List Set

To offer a means of user interaction, the output of WAPP is in the form of a ranked list set of SDs, pitch angles, laminar distances, and effectiveness values. This allows the user to view all SD/SA combinations, not just the recommended one, and select the most appropriate one for the situation. The list set is, therefore, a list of possible presetting choices from which the operator can choose. In addition, the ray traces and signal excess maps are viewable using the GUI's "acoustic coverage" pull-down menu. These forms of output provide a visual interpretation of the acoustic performance of the torpedo, including boundary interactions and refraction effects.

Since the propagation model uses ray theory, it has all the shortcomings associated with it, such as being limited to higher frequencies. In this case, this is an acceptable condition because

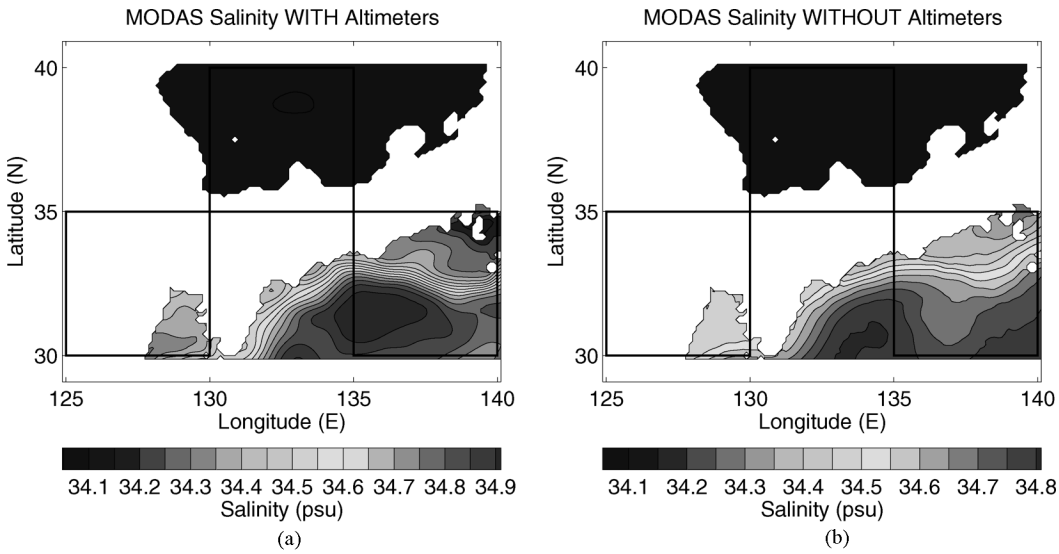

Fig. 8. Comparison between MODAS salinity at 300 m on June 30, 2001 (a) with and (b) without satellite altimetry data assimilated. Here, the upper middle box is used for the SOJ evaluation, the lower right box is used for the KCA evaluation, and lower left box is used for the ECS evaluation (see Fig. 2).

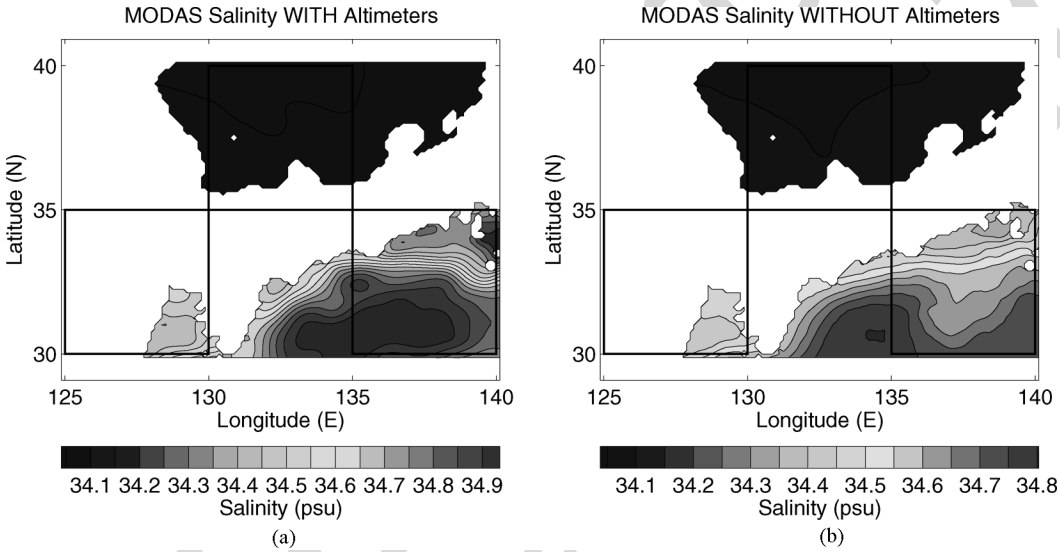

Fig. 9. Comparison between MODAS salinity at 300 m on October 10, 2001 (a) with and (b) without satellite altimetry data assimilated. Here, the upper middle box is used for the SOJ evaluation, the lower right box is used for the KCA evaluation, and lower left box is used for the ECS evaluation (see Fig. 2).

the Mk 48 torpedo has a suitably high operating frequency. Another deficiency of ray theory is the poor handling of shadow zones due to the assumption that no acoustic energy leaks out of the ray tube. This is also acceptable because, from a weapon presetting standpoint, it is unrealistic to direct a torpedo home on a target in a shadow zone, so an accurate description of the sound field is not necessary***[AU: Sentence was changed. Please check.]***. Finally, ray theory has the issue of causing energy to approach infinity at caustics and turning points. This last concern is mitigated through the use of a caustic correction that modifies the propagation equations, thereby avoiding the case where the denominator becomes zero, and approximates the signal level near the caustic.

Because the propagation model is range independent, it assumes cylindrical symmetry, meaning it does not have range-varying properties. The resulting ray traces are assumed to be valid for any direction from the source location, as the model environment looks the same down any bearing [6], [12]. This is not ideal for determining accurate sound-propagation characteristics, especially in regions where the oceanography changes rapidly with horizontal distance, and can affect the weapon presets. Under less variable conditions, this shortcoming would probably have little or no affect on the weapon presets, as the typical Mk 48 torpedo engagement would only involve a few kilometers of ocean. Regardless, there is an effort currently underway to utilize the comprehensive acoustic sonar simulation for range-dependent performance predictions for torpedo presetting. The assumption of range independence is consistent with areas where there is little to no bathymetric variation over torpedo detection ranges and also with cross-slope predictions in more variable environments. Here, it provides a reasonable

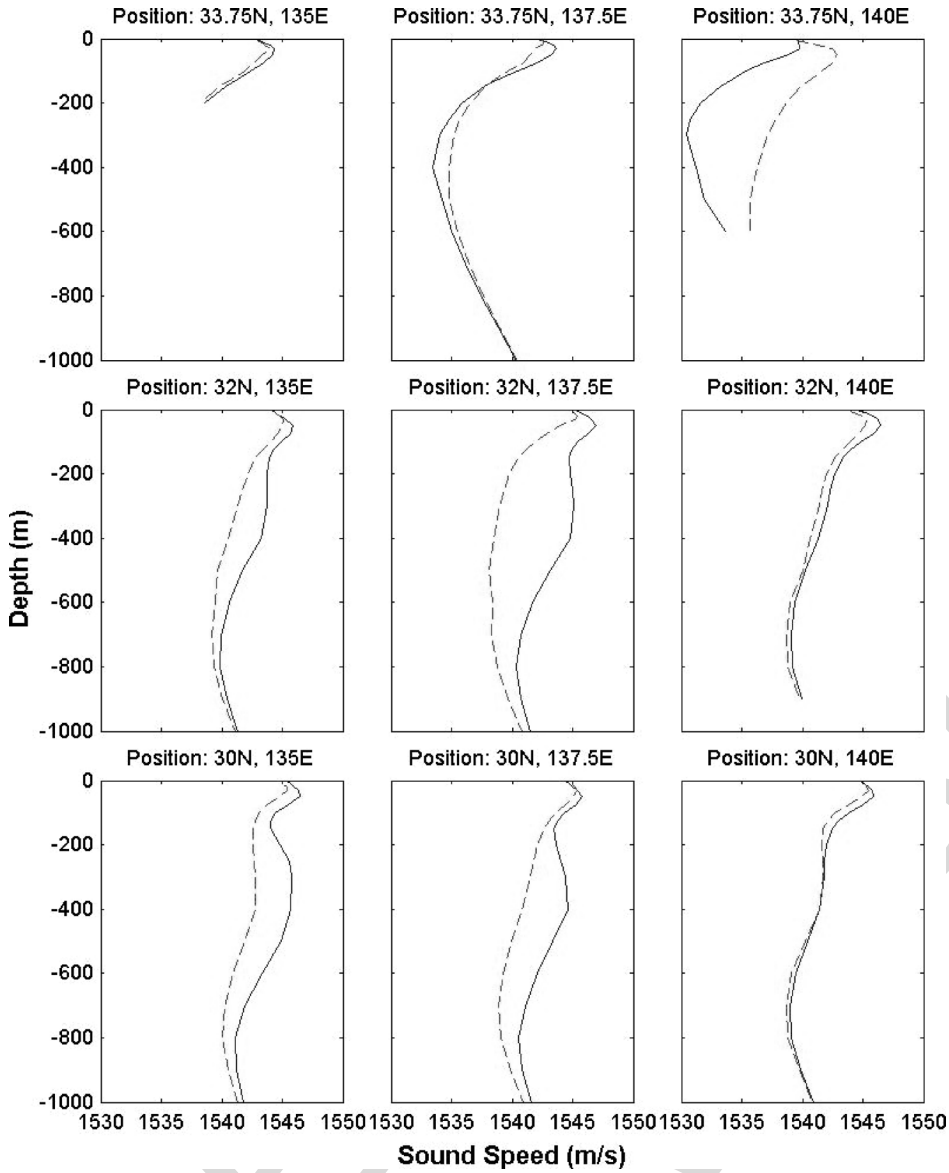

Fig. 10. Comparison of MODAS SSPs for KCA on October 10, 2001 with and without satellite altimetry data assimilated. Here, the solid curves are SSPs with altimeters and the dashed curves are SSPs without altimeters.

assessment of the importance of satellite altimetry data using the current weapon system.

IV. Numerical Simulations

The MODAS temperature and salinity fields were fed into WAPP. Then, WAPP performed its presetting process for each MODAS grid point using the vertical profile data for each location. Grid points over land had no vertical profiles, of course, and are discarded. The vertical SSP is calculated by WAPP from the temperature and salinity profiles, as opposed to using the SSP available from the MODAS field. The same default values for volume scattering strength and surface and bottom roughness/reflectivity were used for each run. This procedure is repeated for the two MODAS field versions (with and without satellite altimetry data), for both days, for each geographic region, and for the five tactical scenarios. The tactical scenarios are prescribed using the GUI to change the tactic ("surface craft" for the ASUW ***[AU: Please define "ASUW"]*** scenarios, "unknown sub" for the ASW scenarios), the target maximum depth (15 m for the ASUW scenarios, 213 m for the shallow ASW scenarios, and 396 m for the deep ASW scenarios), and the target Doppler ("low" for the low Doppler scenarios, "high" for the high Doppler scenarios).

Since one list set is produced for each profile and five different tactical scenarios are integrated for each case, five times as many list sets are produced as there are MODAS profiles. These list sets can be considered as pairs, just as the vertical profiles are; one pair for each location, day, and tactical scenario, each being comprised of one list set for each of the two MODAS field versions. To compare each pair of list sets, a configuration management program and its included statistical software package are employed. This program is actually designed to check WAPP output for differences during verification testing upon completion of software upgrades. In that application, the input is held

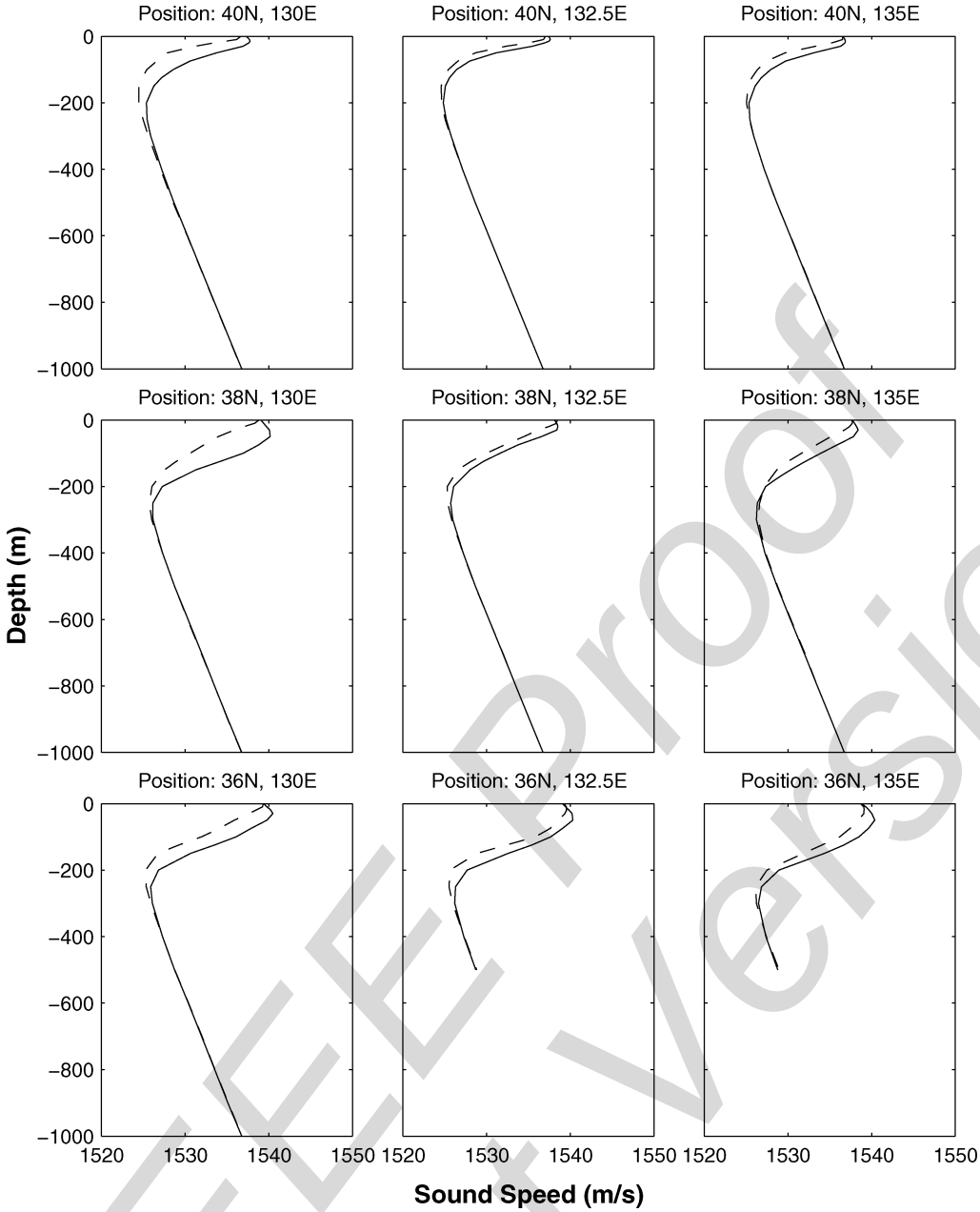

Fig. 11. Comparison of MODAS SSPs for SOJ on October 10, 2001 with and without satellite altimetry data assimilated. Here, the solid curves are SSPs with altimeters and the dashed curves are SSPs without altimeters. The use of SSH data by MODAS introduced only small changes in the SOJ SSPs at weapon/target depths relative to the changes witnessed in the KCA area for the same time period (see Fig. 10). This is a result of larger rmsd of temperature in the KCA than in SOJ especially at depths deeper than 400 m (see Fig. 4).

constant between the two WAPP software versions, so any differences in output are due to software changes (the aim is to have no differences). For the current application, the input was varied and the WAPP version was held constant. Therefore, any differences in the output can be attributed to differences in the input.

V. Statistical Analysis

A. Input and Output Differences

The difference of the two sets of input MODAS with and without satellite altimetry data $(X_1^{(\mathrm{in})}, X_2^{(\mathrm{in})})$ and the two sets of output weapon preset data using MODAS with and without satellite altimetry data $(X_1^{(\mathrm{out})}, X_2^{(\mathrm{out})})$

$$\Delta X = X_1 - X_2$$

represent the ocean data update using satellite altimetry data (input) and the effect of using satellite altimetry data on the weapon preset (output). Here, X_1 and X_2 are the variables (either input or output) using MODAS with and without satellite altimetry data, respectively. The difference was calculated at each horizontal grid point and depth. Besides histograms and scatter diagrams of the two sets of input and output data, bias

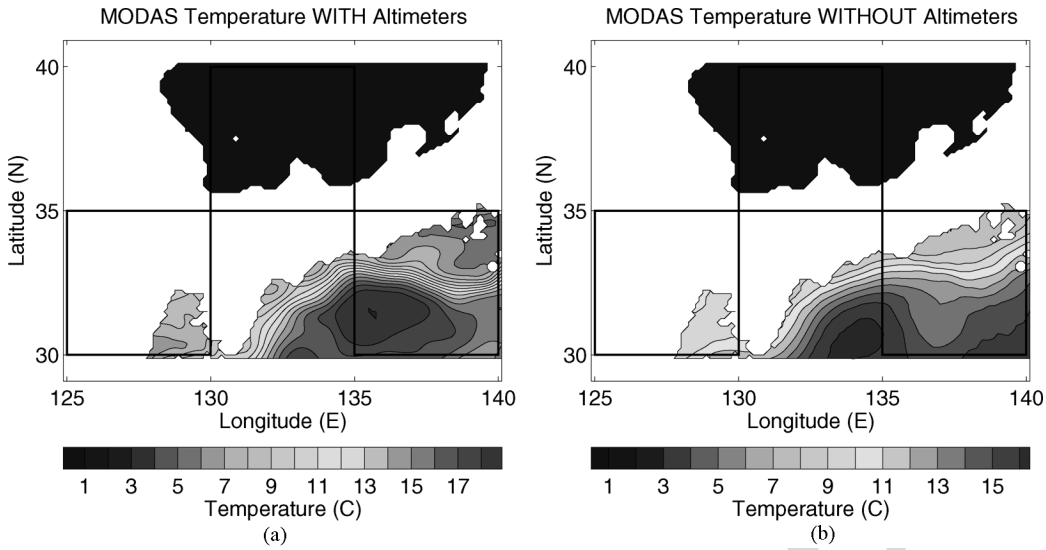

Fig. 12. Comparison between MODAS salinity at 400 m on June 30, 2001 (a) with and (b) without satellite altimetry data assimilated. Here, the upper middle box is used for the SOJ evaluation, the lower right box is used for the KCA evaluation, and lower left box is used for the ECS evaluation (see Fig. 2).

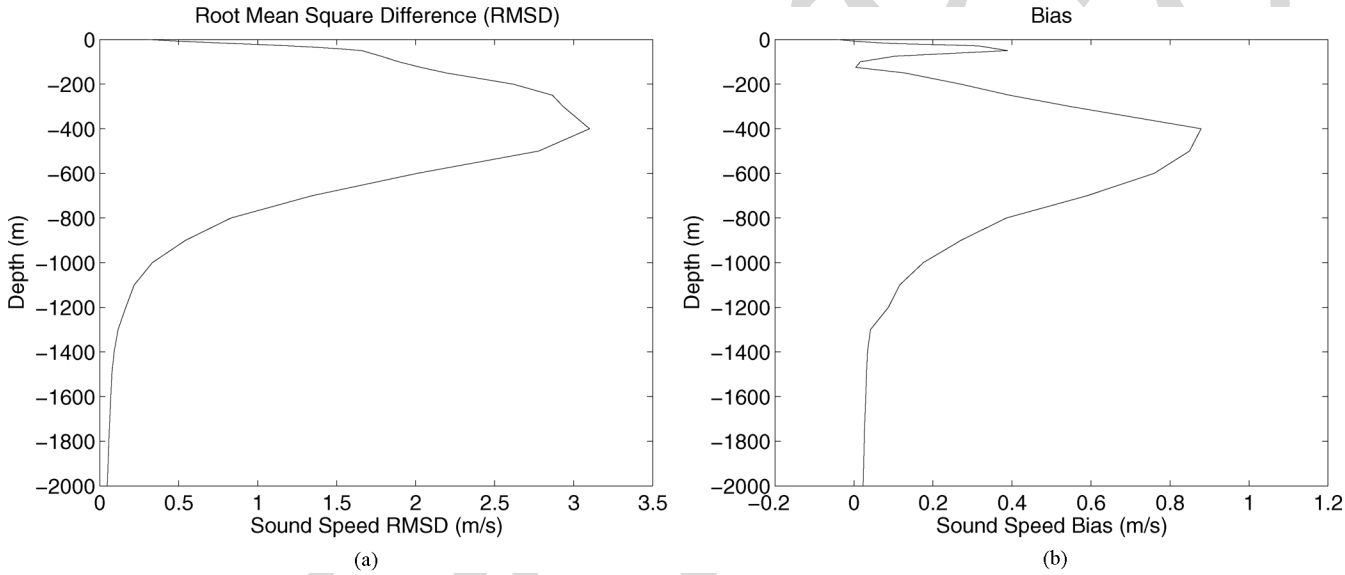

Fig. 13. (a) Horizontal rmsd and (b) bias of MODAS SSP for KCA on June 30, 2001.

and root-mean-square difference (rmsd) are often used. The bias is represented by the mean of the following differences:

$$\Delta\overline{X} = \frac{1}{n}\sum_{i=1}^{n}\Delta X_i \tag{3}$$

and the overall difference is represented by the rmsd

$$\text{rmsd} = \sqrt{\frac{1}{n}\sum_{i=1}^{n}\Delta X_i^2}. \tag{4}$$

Bias and rmsd can be computed over volume (called volume rmsd) or over a horizontal plane (called horizontal rmsd).

B. Probability of Relative Difference Over a Threshold

The statistical package produced absolute values of the relative differences (RD) in area coverage (AC) for different SD/SA combination

$$\text{RD} = \frac{|\text{AC}_1 - \text{AC}_2|}{\text{AC}_1}. \tag{5}$$

Here, the subscripts 1 and 2 denote MODAS with and without satellite altimetry data.

The presetting process has generated pairs of list sets in which some SD/SA combinations were the same and some were different. The list set can be thought of as a list of presetting choices; the choices on one list sometimes match those on the other list and sometimes they do not. The instances in which WAPP produce different SD/SA combinations for a profile pair are the cases in which an actual engagement will have greater

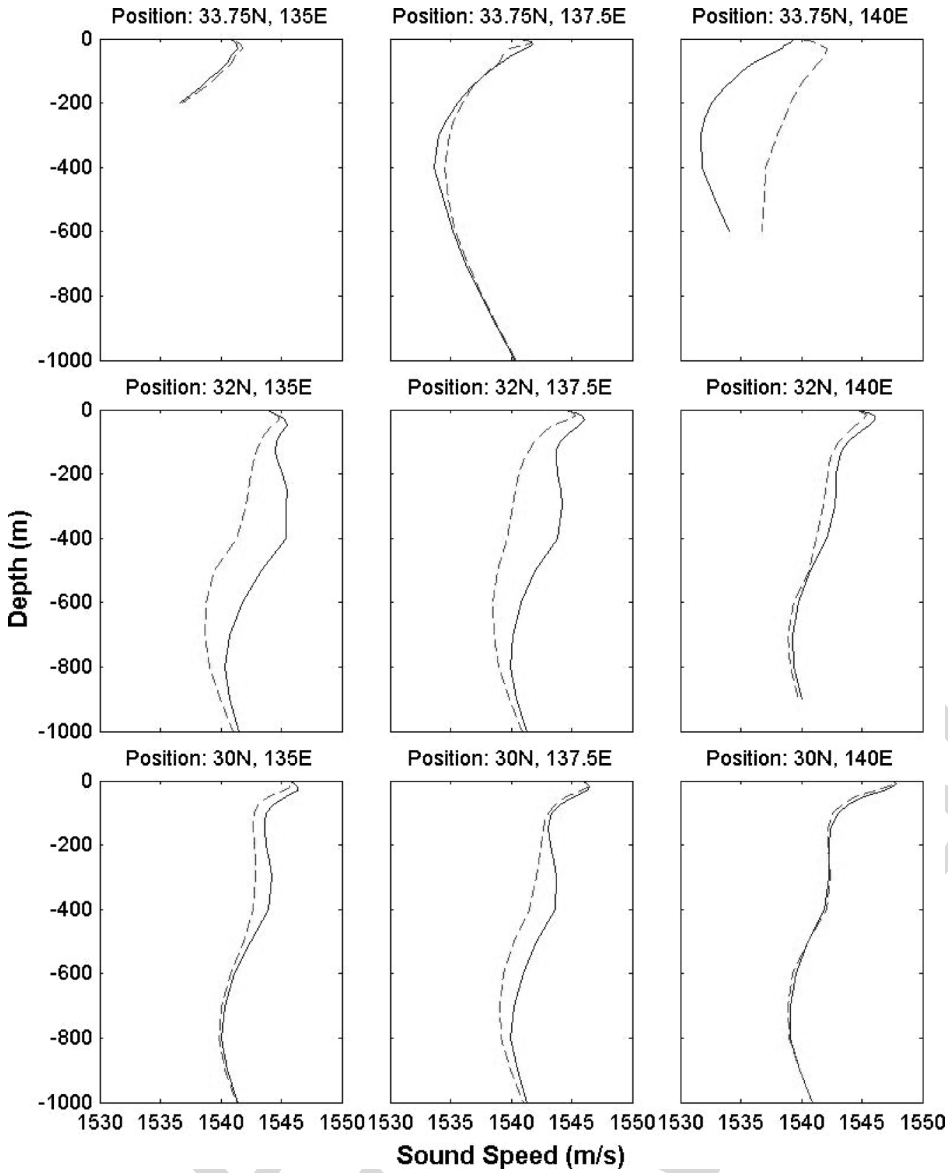

Fig. 14. Comparison of MODAS SSP for KCA on June 30, 2001 with and without satellite altimetry data assimilated. Here, the solid curves are SSPs with altimeters and the dashed curves are SSPs without altimeters.

potential for a different outcome because, given these different choices, the torpedo will not be searching at the same depth, looking at the same SA, or both. Determining the sensitivity of WAPP to input differences in these cases is important because of the potential for weapon effectiveness to be affected. The thing to be aware of here is that the actual environment is whatever it is, regardless of differences in the MODAS fields. In the cases where the same SD/SA combinations (same choices) are generated for the two MODAS versions, the outcome of the engagement will be very similar, subject to other targeting considerations, because the same presets and environment are involved.

Histogram of RD displays the number of different SD/SA combinations with area coverage relative differences in specified ranges, or bins. The probabilities of RD being greater than 0.1, 0.2, and 0.5

$$\mu_1 = \mathrm{Prob}(\mathrm{RD} > 0.1)$$
$$\mu_2 = \mathrm{Prob}(\mathrm{RD} > 0.2)$$
$$\mu_3 = \mathrm{Prob}(\mathrm{RD} > 0.5) \quad (6)$$

are used for the determination of the sensitivity.

VI. Comparison Between Two MODAS Data Sets

A. Volume rmsd

The volume rmsd values (Table I) indicate overall difference in the MODAS analyses for each case. The largest differences in the temperature fields occurred in KCA on both days and in SOJ on October 10, 2001, where the volume rmsd values ranging from 1.58 °C to 1.80 °C. The other cases have rmsd values of 1.18 °C or less. Salinity differences are also largest in KCA on both days, but ECS on June 30, 2001 had large volume salinity rmsd as well. These three cases have values ranging from 0.0759 to 0.0822 psu, whereas the other cases have values of 0.056 psu or less. The derived sound-speed analyses closely followed

the temperature fields, which is to be expected as temperature ranges often have the largest affect on sound speed. The largest values of the sound-speed volume rmsd range from 1.62 to 1.84 m/s and occur in the same cases as they do for the temperature analyses. The remaining cases have values of 1.15 m/s and smaller.

B. Horizontal rmsd

1) MODAS on October 10, 2001: The vertical profiles of horizontal rmsd allow for a more detailed comparison by showing at what depths the largest average differences occurred for each case. The largest differences in the temperature analyses occurred in the October 10 profiles for KCA and SOJ. Both have horizontal rmsd values of well over 3 °C at different depths, as shown in Fig. 4. The maximum values in the KCA profile occur between 300 and 500 m, whereas in the SOJ profile they are in the 50–200-m range.

A comparison of the horizontal temperature fields on October 10, 2001 at 100 m (Fig. 5) and 500 m (Fig. 6) lends some explanation for the high rmsd values in these cases. The panel with altimeter data in Fig. 5 reveals a subsurface eddy system, comprised of both a warm-core and a cold-core eddy, and a stronger polar front in SOJ; eddies are noticeably absent from the panel without altimeter data. The panel with altimeter data in Fig. 6 shows a much stronger subsurface front in KCA, including cooler water to the north and warmer water to the south of the front, than the panel without altimeter data does.

The largest differences in the salinity analyses occur in the KCA profiles on both days. They have horizontal rmsd values of about 0.15 psu or more, with maximum values in the 200–400-m range, as shown in Fig. 7. The horizontal salinity fields at 300 m are shown in Figs. 8 and 9. Similar to the temperature field shown previously, a much stronger front is depicted in the panel with altimetry data, with a larger contrast in salinity on either side of the front. This is true for both days.

As is to be expected, the horizontal rmsd for SSP looks very similar to that for temperature. It follows, then, that the largest values of well over 3 m/s occur in the October 10 profiles for KCA and SOJ at the same depth ranges as the temperature profiles: 300–500 m in the KCA profile and 50–200 m in the SOJ profile.

The horizontal rmsd previously discussed helps to explain the SSP pattern observed for each case. Figs. 10 and 11 illustrate this well for the two cases with the largest differences in the sound-speed (and temperature) MODAS analyses, the October 10 fields for KCA and SOJ. The nine SSP pairs in each figure are displayed so that their positions correspond to their locations within the area. For example, the top left panel shows the SSP pair for a location in the northwest portion of the box; the center panel is for a location near the center of the box, and so on. (Note: the horizontal scale may change from panel to panel, so care must be taken to understand the relative changes between panels.) This type of display provides the additional information of horizontal positioning of the largest differences as well as their depths.

The largest deviations found in the SSP pairs (Fig. 10) correspond to the depth zone already identified as having the largest rmsd values for KCA on October 10, that being 300–500 m. The top-right, center, and two bottom-left panels show the most deviation and correspond to the locations of the largest temperature differences in Fig. 6. The top three panels are profiles from within the front, showing the stronger gradient discovered earlier for the field with altimetry than for the one without. These stronger gradients produce the stronger sound channels evident in the right two panels. The middle and bottom panels show the result of the field with altimetry having much warmer water to the south of the front: the sound speeds are much faster there. They also show more of a gradient in the nonaltimetry field; a result of that field depicting a more spread out front than the tightly packed, stronger front of the altimetry field. Another obvious difference in the center and two bottom-left panels is the second, shallow sound channel in the altimetry field profiles, where one does not exist (or is very weak) in the nonaltimetry field.

Looking now at SOJ on October 10, shown in Fig. 11, the largest deviations in the SSP pairs are seen in the left most panels in the upper 200 m, corresponding to where the eddy system is located in Fig. 5. In all the panels, for the most part, the altimetry profiles show higher sound speeds in the upper 300 m or so, this mostly being due to the prevalent warmer temperatures in the altimetry field there. Very noticeable in the middle and bottom panels is a more pronounced sonic layer at the surface in the altimetry fields, corresponding to the existence of, or a deeper, mixed layer.

2) MODAS on June 30, 2001: Just like on October 10, 2001 (Fig. 6), the temperature field on June 30, 2001 shows a much stronger subsurface front as well as cooler water to the north and warmer water to the south of the front in the MODAS temperature field with altimetry [Fig. 12(a)] than without altimetry [Fig. 12(b)]. The salinity field with altimetry (Fig. 8) also indicates the existence of a stronger front. The largest rmsd of SSP and bias values exist in a band from about 100 to 600 m on June 30, 2001 (Fig. 13). The MODAS SSPs on June 30, 2001 (Fig. 14) illustrate characteristics similar to the SSPs for KCA on October 10, 2001 (Fig. 10).

VII. Comparison of Weapon Acoustic Preset Pairs

The differences in the MODAS fields may have an effect on the output of WAPP, depending on the sensitivity of WAPP to changes in input. The cases highlighted here have fairly significant differences in the temperature, salinity, and sound-speed fields. For the most part, in each of the 30 scenario histograms, the number of different SD/SA combinations dropped off with increasing RD. In other words, the peak RD was usually in the lowest bin (less than 0.05) and decreased with each successive bin in a decaying fashion, as illustrated by Fig. 15(a). The most notable exceptions are the two ASUW tactics for the SOJ October case, which have peaks in the bin for 0.3–0.4, one of which is shown in Fig. 15(b). The next two figures ***[AU: Please specify which figures]*** display collectively some of the values determined for each histogram, including μ_1 and μ_2 (i.e., the probabilities of the RD being greater than 0.1 and 0.2) and mean RD. The results are grouped by case and broken down into each tactic.

The general trend for each case (except for SOJ on June 30, 2001) is for the probability values to decrease with increasing

TABLE II
OVERALL SENSITIVITY OF WEAPON ACOUSTIC PRESET TO ALTIMETRY DATA ASSIMILATION USING MODAS

Scenario	Prob(RD > 0.1)	Prob(RD > 0.2)	Prob(RD > 0.5)	Mean RD
ECS Jun HD Deep ASW	17.51	2.64	0.00	0.0618
ECS Jun LD Deep ASW	21.82	4.10	0.00	0.0725
ECS Jun LD Shallow ASW	21.77	3.65	0.00	0.0723
ECS Jun HD ASUW	39.59	19.63	0.28	0.1110
ECS Jun LD ASUW	26.29	9.45	0.06	0.0818
KCA Jun HD Deep ASW	39.26	6.63	0.00	0.0924
KCA Jun LD Deep ASW	37.52	6.44	0.00	0.0925
KCA Jun LD Shallow ASW	46.76	8.46	0.00	0.1020
KCA Jun HD ASUW	55.98	30.19	0.05	0.1450
KCA Jun LD ASUW	43.62	17.20	0.04	0.1090
SOJ Jun HD Deep ASW	17.50	2.86	0.00	0.0616
SOJ Jun LD Deep ASW	18.91	3.03	0.00	0.0623
SOJ Jun HD Shallow ASW	11.63	1.20	0.00	0.0509
SOJ Jun HD ASUW	2.43	0.47	0.00	0.0396
SOJ Jun LD ASUW	1.43	0.34	0.00	0.0382
ECS Oct HD Deep ASW	8.11	0.42	0.00	0.0472
ECS Oct LD Deep ASW	11.83	1.09	0.00	0.0520
ECS Oct HD Shallow ASW	15.36	4.71	0.00	0.0611
ECS Oct HD ASUW	49.23	13.99	0.00	0.1100
ECS Oct LD ASUW	51.90	25.39	0.99	0.1420
KCA Oct HD Deep ASW	35.68	4.53	0.00	0.0861
KCA Oct LD Deep ASW	33.48	3.38	0.00	0.0834
KCA Oct HD Shallow ASW	50.74	8.34	0.00	0.1060
KCA Oct HD ASUW	43.63	8.51	0.02	0.0997
KCA Oct LD ASUW	47.49	6.93	0.07	0.1030
SOJ Oct HD Deep ASW	29.61	5.11	0.00	0.0793
SOJ Oct LD Deep ASW	26.55	4.41	0.00	0.0777
SOJ Oct HD Shallow ASW	36.71	8.79	0.00	0.0921
SOJ Oct HD ASUW	91.45	84.11	1.82	0.3030
SOJ Oct LD AUW	81.77	62.30	1.01	0.2410

tactic depth band (Table II). In other words, one or both ASUW tactics tended to have the highest probability values followed by the shallow ASW tactic, with the deep ASW tactics having the lowest probability values. Interestingly, this trend is reversed for the SOJ on June 30, 2001. The other obvious tendency is for the values of μ_1 to be several times greater than the values of μ_2, reiterating the decaying pattern.

The highest μ_1 is 91.5%, attained by the high Doppler ASUW tactic in the SOJ October case. The low Doppler ASUW tactic in the same case also has a high value at 81.8%. The next high values are in the 50% range. The same two scenarios also achieved the highest μ_2, with 84.1% and 62.3%, respectively. The next high values are about 30% or lower. Only nine of the histograms had nonzero μ_3 [i.e., $\mathrm{Prob}(\mathrm{RD} > 0.5)$] values (not shown in Table II), all of them being for ASUW tactics, the largest of which is 1.8%. These scenarios with high probability values are the ones in which the outcome of an engagement will most likely be different because they have a higher chance of having large differences in predicted performance.

The lowest μ_1 is 1.4%, attained by the low Doppler ASUW tactic in the SOJ on June 30, 2001. The high Doppler ASUW tactic in that case also has a very low value of 2.4%. The next lowest is 8.1%, three times more than the minimum probability. The same two scenarios also achieved two of the lowest μ_2, 0.3% and 0.5%, respectively. The high Doppler deep ASW tactic for ECS on October 10, 2001 has the other lowest value of 0.4%. The next lowest values are more than 1%. These scenarios with low probability values are the ones least likely to have had an impact on engagement outcome because they have a very low chance of having large differences in predicted performance.

The mean RDs decreased with tactic depth band (Table II), except for the SOJ on June 30, 2001. This pattern makes sense since scenarios with a higher mean RD would be expected to have a higher probability of having larger relative differences. The highest mean RDs are 0.303 and 0.241, attained again by the high and low Doppler ASUW tactics in the SOJ on October 10, 2001. The next highest are less than 0.15. The lowest mean RDs are 0.0382 and 0.0396, attained again by the low and high Doppler ASUW tactics in the SOJ on June 30, 2001. The next lowest is 0.0472.

For the deeper-based tactics, at least three factors seemed to influence the amount of relative difference in the WAPP output. The first is the peak value of the horizontal rmsd of the MODAS SSP, which causes high values of the mean RD, μ_1 and μ_2. The second factor is the depth of this peak. A deeper depth of the rmsd peak leads to higher WAPP output values. Finally, the shape of the peak played a partial role, as the higher values can also be associated with broader peaks vice narrower ones. The cases with the obviously larger values in Table II, which shows WAPP output values for both of the deep ASW tactics, are the SOJ on October 10, 2001 and the KCA on June 30 and October

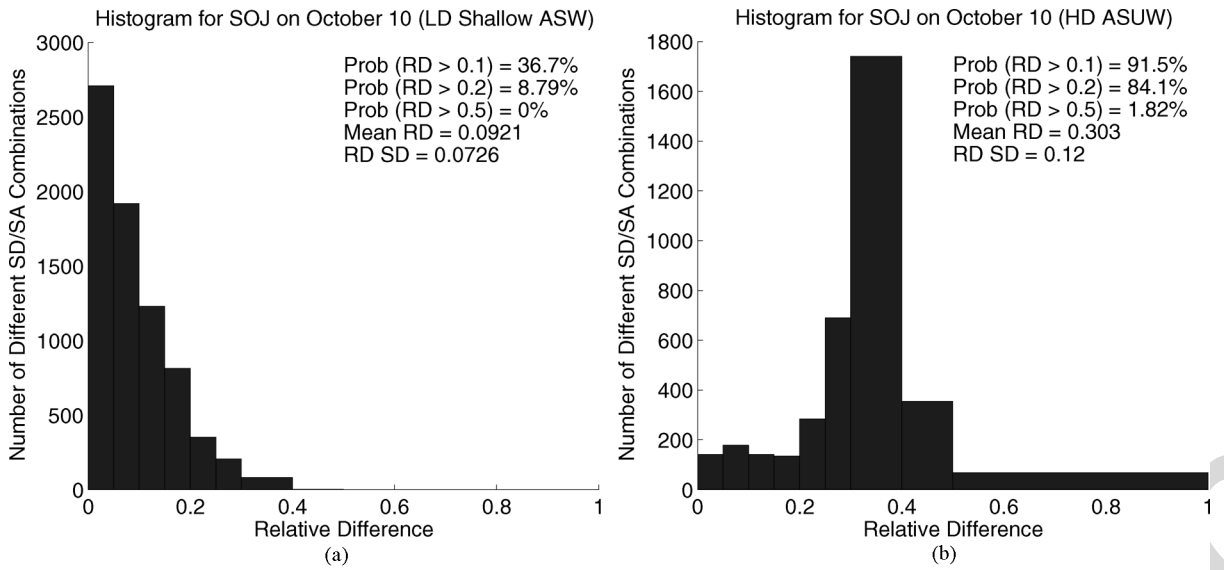

Fig. 15. Histogram of RD of weapon acoustic presets in SOJ for the (a) low Doppler shallow ASW and the (b) high Doppler ASUW.

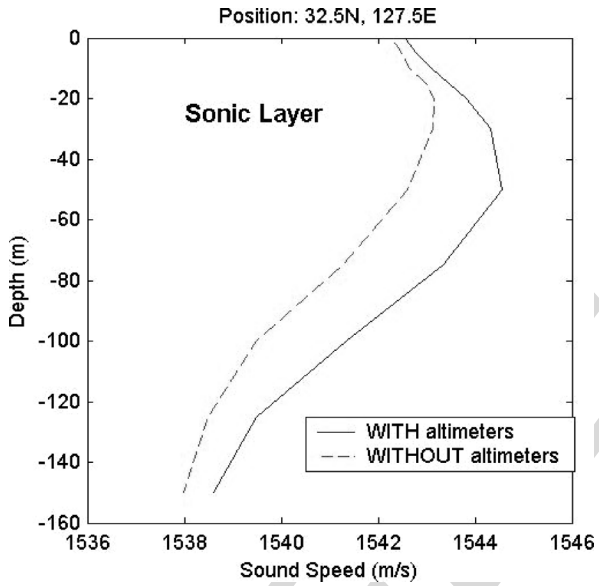

Fig. 16. Comparison of MODAS SSP at 32.5° N, 127.5° E on October 10, 2001 with and without satellite altimetry data assimilated. Note the existence of a sonic layer.

10, 2001 (the same is true for the shallow ASW tactic). All three of these have one or more of the aforementioned factors in their favor.

These results can be understood using Fig. 4, the horizontal rmsd for KCA on October 10, 2001, which shows 2-m/s or larger values occurring in a band from about 100 to 700 m. This band encompasses much of the depth zones of interest for both the deep and shallow ASW tactics (down to about 400 and 200 m, respectively). The MODAS SSPs in Fig. 10 further illustrate the large differences in SSP at these depths. The larger these differences (higher the rmsd peak value) are and the more they extend into the depth zone of interest (owing to the depth and shape of the peak), the larger the difference in the predicted sound propagation for the two MODAS fields in that depth zone is, thus leading to the large probability and mean RD values in WAPP's output for the ASW tactics.

VIII. Overall Sensitivity

From the preceding discussion it is apparent that, in some of the scenarios, WAPP output was quite sensitive to changes in input environmental fields, such as MODAS with satellite altimetry data assimilated versus MODAS without altimetry data. Table II also shows a compilation of the probability values for each scenario, grouped by case, in an effort to more easily compare the sensitivities of each scenario. The μ_1 values range from 1.4 to 91.5 and the μ_2 values range from 0.3 to 84.1, which suggest that the sensitivity of WAPP is extremely variable and, therefore, so is the chance of affecting the outcome of an engagement. Although the ranges are large, most of the 30 scenarios are in the lower halves of them; only one sixth has μ_1 values greater than 50%, one third has values greater than 40%, just over half has values greater than 30%, and only one tenth of the scenarios has μ_2 values greater than 30%. Based on this sensitivity analysis, the satellite altimetry data contributed as much as an 80%–90% chance of having a different engagement outcome (once again, assuming 0.1–0.2 is enough of a relative difference in area coverage to change the outcome), but in most of the scenarios the contribution is less than 50%.

IX. Physical Mechanisms

A. Sonic Layer

A sonic layer occurs when the sound speed increases with depth from the surface to a maximum and then decreases with depth (Fig. 16). A stronger sonic layer would have two effects on near-surface sound-propagation characteristics. If the sound source were in the layer, it would more effectively trap the sound energy by refracting it back to the surface, where it would be reflected back into the water, allowing it to travel greater distances before being diminished. For a source below the layer, it would more effectively prevent sound energy from penetrating

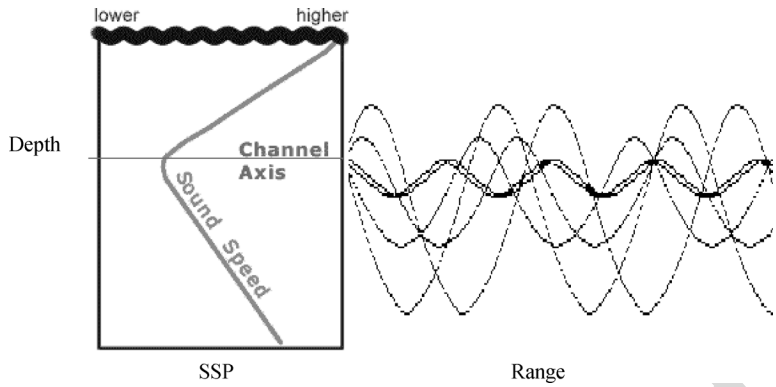

Fig. 17. Sound channel depiction.

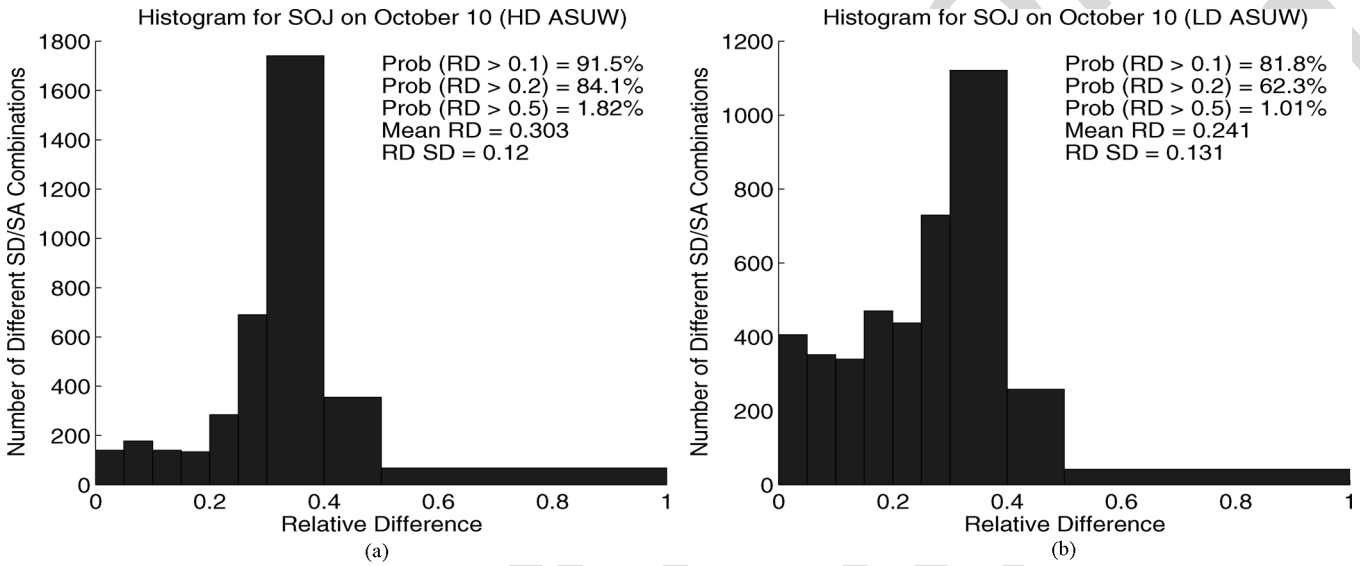

Fig. 18. Histogram of RD of weapon acoustic presets in SOJ for (a) high Doppler shallow ASW and (b) low Doppler ASUW on October 10, 2001.

into it by refracting it down away from the layer, creating a relatively sound-free layer near the surface. Because only one of the MODAS fields produced these effects in each case, the sound-propagation characteristics near the surface would differ substantially resulting in equally dissimilar predictions of sound propagation. This is what led to more significant differences in the presets that WAPP produced for the shallower-based tactics.

B. Sound Channel

One reason for the differences in the ASW scenarios is the existence of sound channels. Sound channels exist when sound speed first decreases with depth and then increases again (see Fig. 17). This produces a refractive environment that focuses the sound energy in a depth band about the channel axis, due to bending above and below the axis. This focusing allows the sound to be detectable at longer distances than it otherwise would because it is less spread out and, thus, more intense. When a sound channel exists or is stronger in one MODAS field, the channeling effect produces significant differences in sound propagation between the two fields.

C. Two Extreme Cases

The two cases with the largest relative differences in WAPP area coverage for ASUW and ASW tactics deserve a closer look: the SOJ on October 10, 2001 for the ASUW tactics and the KCA on June 30, 2001 for the ASW tactics. The former case is examined in detail during the MODAS discussion. Recall that rmsds greater than 3 °C existed in a band from 50 to 200 m due to both a subsurface eddy system and a stronger SOJ polar front. These produced large differences in the SSPs in this depth band (Fig. 11) and associated large horizontal rmsd temperature [Fig. 4(b)]. This shows a very pronounced sonic layer over much of the SOJ region in the MODAS field with satellite altimetry data, but almost no such layer in the MODAS field without satellite altimetry data.

As discussed earlier, the effect of the sonic layer would be to cause WAPP to generate very different near-surface sound-propagation predictions for the two MODAS fields, leading to the large relative differences in area coverage. In the histograms for the two ASUW tactics, shown in Fig. 18, the radically displaced relative difference peaks (in the bin for 0.3–0.4) as compared to the rest of the histograms are apparent. Once again, these two scenarios had the highest probability values and mean

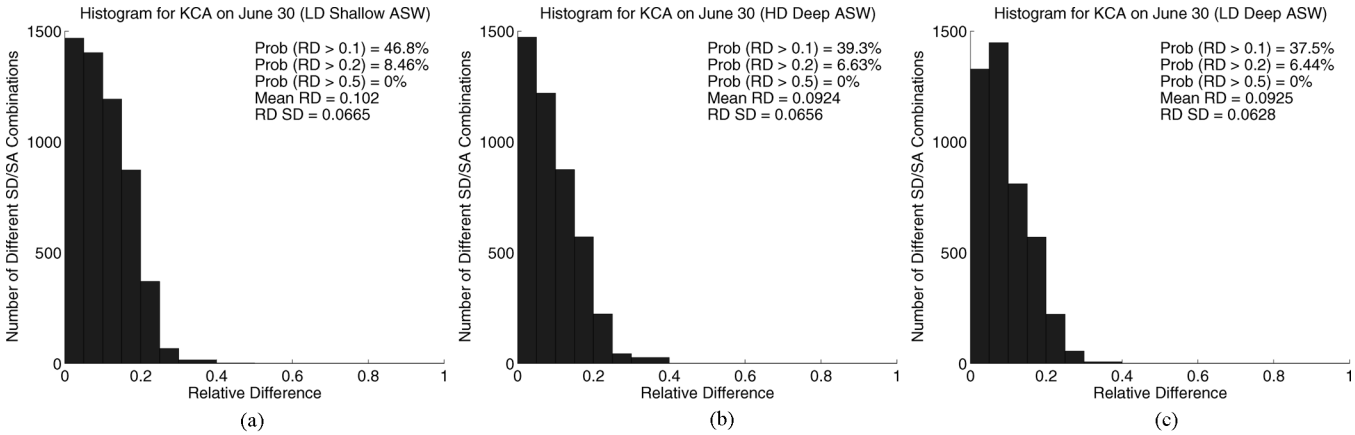

Fig. 19. Histogram of RD of weapon acoustic presets in SOJ for (a) high Doppler shallow ASW, (b) low Doppler deep ASW, and (c) high Doppler deep ASW on June 30, 2001.

RDs of all the scenarios, not just the ASUW ones, and so were very likely to have a different outcome in an actual engagement.

The much larger differences seem to be due to the extra large differences in the MODAS fields. Fig. 11 shows that the sonic layer in the altimetry field is very strong, with sound speed increasing by several meters per second over the depth of the layer in several locations. Some of the other scenarios have equally strong sonic layers, but only in one or two locations. The other big difference that sets these two scenarios apart from the rest is that the other MODAS field (nonaltimetry, in this case) had no appreciable sonic layer anywhere in the region. The other scenarios with strong sonic layers in one field also have a weaker sonic layer in the other field, which helps to offset the difference and apparently limit the effect on WAPP's output.

Shifting now to the largest WAPP output differences for ASW tactics, the KCA on June 30, 2001 just edge out that on October 10, 2001 in the same region***[AU: this sentence is unclear. Please rewrite]***. These two cases have very similar MODAS fields, as discussed in Section VI, and they are both mentioned earlier as having all three influencing factors in their favor: a high sound-speed rmsd peak value, a peak axis well into the depth zone of interest, and a broad peak increasing the extent of the high rmsd values throughout most of the zone of interest.

As discussed for the general case, this depth zone includes most of the ASW zone of interest. Therefore, the predicted sound propagation for the two MODAS fields in the ASW zone was more dissimilar, thus leading to the large differences in WAPP's output for the ASW tactics.

The large differences in the sound-speed fields in the ASW depth zone of interest are partially due to the MODAS field with altimetry having a stronger sound channel, evident in the top-right two panels, which are produced by the stronger frontal gradients in that MODAS field for June 30, 2001 (Fig. 14) and October 10, 2001 (Fig. 10). Another contribution to the sound-speed differences in the ASW band can be seen in the four bottom-left panels, which show a second sound channel with an axis near 100 m in the altimetry field profiles, where one does not exist (or is very weak) in the nonaltimetry field. As discussed earlier, these sound channels would refract sound in a way that would significantly affect sound propagation and, therefore, the output of WAPP when using this MODAS field. The outcome of an engagement would probably have been significantly different, depending on which MODAS field was used. For completeness, the histograms for the three ASW tactics are shown in Fig. 19.

X. Conclusion and Recommendations

The scenarios in which WAPP is the most sensitive are the ones where the input MODAS fields differed significantly, especially in the depth zone of interest for the given tactic. The MODAS fields usually differed in their depiction of mesoscale features, such as eddy systems (e.g., in SOJ on October 10, 2001) and subsurface fronts (e.g., in KCA on June 30 and October 10, 2001), due to only one field having the benefit of satellite altimetry data to help MODAS resolve them. This causes differences in the SSP characteristics for the two fields, such as the sonic layer being more pronounced, sound channels being stronger and, in some cases, one of the fields having no sonic layer or having secondary sound channels. Quite expectably, this led to large differences in the sound-propagation predictions made by WAPP for the two fields, and thus to large relative differences in area coverage.

The most accurate way to assess the satellite altimetry data's overall value is to relate it to how it would affect the outcome of an actual engagement, or weapon effectiveness. The value could then be based on whether the outcomes were affected positively, which in an ASW engagement typically means the torpedo hit the target versus missed it. In this paper, torpedo performance in the real world is not readily quantifiable because, although the MODAS field with satellite altimetry is certainly closer to the actual environmental conditions, neither field can be considered as being the actual environment like an *in situ* measurement can (within the accuracy of the device used). Therefore, there is no way to relate the performance predictions to the expected real-world performance. (The only real-world performance assertion is made to single out the different SD/SA combinations for the sensitivity analysis, namely that the engagement will be very similar if the weapon is assigned the same presets, regardless of which MODAS field is used). Also, a relative difference in area coverage of 0.1 to 0.2 was arbitrarily chosen for analysis,

although higher or lower levels of difference may actually be necessary to affect engagement outcome.

To quantify the effect on weapon effectiveness, a two-part study needs to be conducted. Part 1 compares the output of WAPP using MODAS fields (one with altimetry data and one without, as done here) and *in situ* measurements of the local environment. The *in situ* measurements can be performed by any number of assets, such as a U.S. Navy ship during an exercise or a research vessel, although the area should be one with large variability, such as in the Gulf Stream or Kuroshio Current, to obtain the most benefit from the altimetry data. Of course, as with any experiment involving *in situ* measurements, the data set will be much smaller than the one used in this study.

With this type of comparison, any differences in WAPP output could be correlated to the torpedo's predicted real-world performance and, therefore, so could the benefit of the satellite altimetry data. For example, if the predicted performance is similar for the MODAS field with altimetry and the *in situ* data, but the performance differed appreciably for the MODAS field without altimetry, the altimetry data would be quite valuable. If the predicted performance differed appreciably between all three inputs or between the *in situ* input and both MODAS fields, the altimetry data would be deemed as being less beneficial. However, the predicted performance is still not a real-world performance.

To assess the effect of the satellite altimetry data on weapon effectiveness even better, part 2 needs to include simulations of torpedo engagements. The Weapons Analysis Facility at NUWC, Division Newport has the capability to simulate engagements using torpedo hardware-in-the-loop and a high-fidelity virtual environment. Using the Weapon Analysis Facility and presets generated by the MODAS fields and the *in situ* data in part 1, many virtual torpedo engagements can be conducted to examine the effects of the different MODAS fields on virtual performance. This can be done for any number of scenarios, by alternately using presets generated by each of the environmental inputs to WAPP: the MODAS field without altimetry, the MODAS field with altimetry, and the *in situ* data; and then, comparing the ratios of hits to misses for the virtual engagements.

This experiment introduces an operational element by enabling the presets to be chosen by an operator for each engagement. It also eliminates the need to use the relative difference in area coverage and the associated uncertainty in the threshold that produces changes in engagement outcome. This is because the proposed metric, the hit–miss ratio, is not a prediction of performance (like area coverage) but, rather, a direct assessment of it (once again, in a virtual environment). Aside from the cost and logistics prohibitive alternative of putting many torpedoes in the water, an experiment such as this would provide the next best analysis of the value of assimilating satellite altimetry data into MODAS with regard to torpedo effectiveness.

Finally, to arrive at answers to some of the broader questions in this line of research, other comparisons need to be included. These are the questions of how many satellite altimeters are required to ensure maximum weapon effectiveness and at what point additional altimeter input no longer increases weapon effectiveness. To answer these questions, MODAS fields with varying number of altimeters assimilated would need to be used as environmental inputs to WAPP and could be incorporated into part 1 or added at a later date.

REFERENCES

[1] M. R. Carnes, D. Fox, and R. Rhodes, "Data assimilation in a north Pacific ocean monitoring and prediction system," in *Modern Approach to Data Assimilation in Ocean Modeling*, P. Malanote-Rizzoli, Ed. New York: Elsevier, 1996, pp. 319–345.

[2] M. R. Carnes, L. Mitchell, and P. W. deWitt, "Synthetic temperature profiles derived from Geosat altimetry: Comparison with air-dropped expendable bathythermograph profiles," *J. Geophys. Res.*, vol. 95, no. C10, pp. 17 979–17 992, 1990.

[3] C. T. Chen and F. J. Millero, "Speed of sound in seawater at high pressures," *J. Acoust. Soc. Amer.*, vol. 62, pp. 1129–1135, 1977.

[4] P. C. Chu, M. D. Perry, E. L. Gottshall, and D. S. Cwalina, "Satellite data assimilation for improvement of naval undersea capability," *Marine Technol. Soc. J.*, vol. 38, no. 1, pp. 11–23, 2004.

[5] P. C. Chu, W. Guihua, and C. Fan, "Evaluation of the U. S. Navy's modular ocean data assimilation system (MODAS) using south china sea monsoon experiment (SCSMEX) data," *J. Oceanography*, vol. 60, pp. 1007–1021, 2004.

[6] P. C. Etter, *Underwater Acoustic Modeling: Principles, Techniques and Applications*. New York: Elsevier, 1991, p. 305.

[7] D. N. Fox, W. J. Teague, C. N. Barron, M. R. Carnes, and C. M. Lee, "The modular ocean data assimilation system (MODAS)," *J. Atmos. Ocean. Technol.*, vol. 19, pp. 240–252, 2002.

[8] D. N. Fox, C. N. Barron, M. R. Carnes, M. Booda, G. Peggion, and J. Gurley, "The modular ocean data assimilation system," *Oceanography*, vol. 15, pp. 22–28, 2002.

[9] R. E. Francois and G. R. Garrison, "Sound absorption based on ocean measurements. Part 1: Pure water and magnesium sulfate contribution," *J. Acoust. Soc. Amer.*, vol. 72, pp. 896–907, 1982.

[10] ——, "Sound absorption based on ocean measurements. Part 2: Boric acid contribution and equation for total absorption," *J. Acoust. Soc. Amer.*, vol. 72, pp. 1879–1890, 1982.

[11] ***[AU: Please provide department]***S. Mancini, "Sensitivity of satellite altimetry data assimilation on a naval anti-submarine weapon system," M. S. thesis, Naval Postgraduate School, Monterey, CA, 2004.

[12] H. Medwin and C. S. Clay, *Fundamentals of Acoustic Oceanography*. New York: Academic, 1997, p. 712.

[13] P. J. Washburn, "MODAS – The warfighters' view of the undersea environment," *NMOC News*, vol. 24, p. 2, 2004.

Peter C. Chu received the Ph.D. degree in geophysical fluid dynamics from the University of Chicago, Chicago, IL, in 1985.

He is a Professor of Oceanography and Head of the Naval Ocean Analysis and Prediction (NOAP) Laboratory, the Naval Postgraduate School, Monterey, CA. His research interests include ocean analysis and prediction, coastal modeling, littoral zone oceanography for mine warfare, mine-impact burial prediction, mine acoustic detection, and satellite data assimilation for undersea warfare.

Steven Mancini was born in Cincinnatti, OH, on April 21, 1971. He received the B.S. degree in applied physics from Xavier University, Cincinnatti, OH, in 1992 and the M.S. degree in meteorology and physical oceanography from the Naval Postgraduate School, Monterey, CA, in 2004.

Since November 2004, he has been present METOC/Asst. Surf. Ops/Scheduler ***[AU: Please define "METOC" and spell out the title]*** at the Commander Carrier Group Seven, North Island, CA. From June 1992 to September 1992, he was a Student at the Officer Candidate School, Newport, RI. From October 1992 to April 1993, he was a Student at the Naval Nuclear Power School, Orlando, FL. From May 1993 to November 1993, he was a student at the NPTU Idaho Falls, ID. From December 1993 to May 1994, he was a Student at the Surface Warfare Officer School, Newport, RI. From June 1994 to June 1996, he was with the Reactor Department, U.S.S. Enterprise (CVN 65), Norfolk, VA. From July 1996 to September 1997, he was with the Combat Systems Department, U.S.S. Saipan (LHA 2), Norfolk,

VA. From October 1997 to September 1999, he was with the C4I Department, Commander Operational Test and Evaluation Force, Norfolk, VA. From October 1999 to December 1999, he was a Student at the Basic Oceanography Accession Training, Gulfport, MS. From January 2000 to June 2002, he was with the Operations Department, Naval Pacific Meteorology and Oceanography Center, San Diego, CA. From July 2002 to October 2004, he was a Student at the Naval Postgraduate School, Monterey CA.

Eric L. Gottshall received advanced degrees in physics and meteorology and physical pceanography.***[AU: what degrees, in what year and from what university?]***

He is an Active Duty Navy Oceanographer currently assigned as an Associate Director for Ocean, Atmosphere, and Space Sciences at the Office of Naval Research Global, London, U.K. ***[AU: This affiliation does not match the one on p.1. Please advise.]***He is the Defense Acquisition Workforce Level III certified in systems planning, research, development, and engineering. He is a member of the Navy's Space Cadre

David S. Cwalina was born in Peabody, MA, on November 9, 1957. He received the B.S. degree in physics from the University of Massachusetts, Lowell, in 1979, the M.S. degree in computer and systems engineering from Rensselaer Polytechnic Institute, Troy, NY, in 1982, and the M.S. degree in electrical engineering from the University of Rhode Island, Kingston, in 1992.

In 1982, he joined the Naval Underwater Systems Center (now Naval Undersea Warfare Center) in the Combat Control Systems Department. Currently, he works in the areas of torpedo and unmanned vehicle engagement planning, modeling and simulation, guidance and control, and performance prediction.

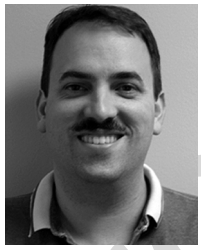

Charlie N. Barron received the Ph.D. degree in oceanography from Texas A&M University***[AU: Location?]*** in 1994.

He is an oceanographer at the U.S. Naval Research Laboratory, Stennis Space Center, MI, specializing in global ocean modeling and data assimilation.